

Authors' Note to the Associate Editor and Reviewers

Title: Sensitivity of Uncertainty in Wind Characteristics and Wind Turbine Properties on Wind Turbine Extreme and Fatigue Loads

Ref. No: wes-2019-2

The authors thank the reviewers for their thorough assessment, comments, and insights. Revisions are shown in the updated version of the paper below with Track Changes.

Reviewer's comments are shown below in blue. Authors' responses are shown in black.

Reviewer 1

The date of Reference number 2 ("Assessment of extreme design loads for modern wind turbines using the probabilistic approach," DTU Wind Energy (DTU Wind Energy PhD; No. 0048(EN)) should be 2015 and not 2018.

A. This has been corrected in the reference itself and any mention of the reference throughout the paper.

Early in the paper, the authors should consider explaining their logic for choosing to use the Elementary Effects sensitivity approach instead of other approaches. As far as I am concerned EE sensitivity type of analysis is mainly used for initial assessments of input parameters, when you have large number of input parameters and it only provides information in the qualitative sense: indicates influential vs non-influential input, and hints to higher order effects caused by nonlinear or interactive relationship between parameters. You briefly explain this in section 3.1, but maybe you should consider summarizing the logic in your intro.

A. We have added some new information to the introduction based on this advice.

Page 2, Lines 4-6: I don't fully agree. Say we have a long and slender blade. You use ElastoDyn for the to define the blade dynamics via 1-2 assumed flap and 1-edge modes. This means that all your structural dynamics are effectively filtered through those three modes. A complex combination of wind speed, turbulence, shear, veer and yaw error might -in reality- result in a bend-twist coupling that will increase the loads or, unintuitively, reduce the loads (because the twist results in lower angles of attack). You will never be able to capture such a phenomena with a simpler model resulting in erroneous conclusions on your sensitivity analysis.

A. It has been shown in many studies that ElastoDyn is sufficiently accurate for loads analysis of the NREL 5 MW turbine blade. This has been shown via code-to-code comparisons to BeamDyn, MSC.ADAMS, HAWC2, Bladed, etc.

Page 2, Lines 13-14: What do you see the downfall of your sensitivity analysis if correlations and joint distributions of input parameters are not taken into account? See for instance slides 22 and 23 in <http://www.gdr-mascotnum.fr/media/mascot12caniou.pdf>

A. Correlations and joint distributions of the parameters were not considered since developing this relationship for so many parameters would be difficult or impossible. In addition, the correlation could be very different for different wind sites. The impact of not considering the correlation was limited by choosing parameters that were fairly independent of one another, when possible, and by binning the results by wind speed.

On the same topic, since you use ranges, you might easily fall into an erroneous case where high wind speeds and large shear exponents ($\alpha > 1$) combine ... but I could see from Table 3 that you chose your ranges and combinations carefully (you also make this clear on lines 4.8, page 10).

A. The authors agree and correlations on inflow parameters were minimized by binning the results by mean wind speed.

Page 3, Lines 23-24: could you please explain the reason for choosing the vector sum of the components of the bending moments? Imagine bending moment M_x is an order of magnitude larger than bending moment M_y . Under some combination of the input, we observe that M_y exhibit large variations ($\times 2$ or $\times 3$) whereas M_x doesn't. However, given that M_x is an order of magnitude larger than M_y , the large fluctuations of M_y will not be really reflected in the vector sum. Consequently, the sensitivity analysis will not reflect the real effects of the input any longer.

A. It is common practice in axisymmetric structure responses (blade root, drivetrain, tower) to only consider the vector magnitude of the bending moments in ultimate loads analysis.

Page 10, lines 4-6: I actually propose you compare the sensitivity analysis performed on the same set of input assuming they are independent and then assuming joint distributions (where possible).

A. It would not be possible to make an 18-dimensional joint probability distribution. The purpose of this study is to take a very large set of input parameters and identify the parameters that most contribute to turbine response sensitivity. As such, including 18-dimensional joint distributions is not possible and was not considered for the present study. However, it would be beneficial to include joint probability distributions in future studies that include fewer parameters.

Despite my previous comment, your results in Figures 3 & 4 and your summary on page 18, conform to results found by investigators/researchers. So, I don't think you have introduced flagrant errors using the approach proposed in this article.

A. Agreed.

Section 4.2.2.4 Steady Airfoil Aerodynamics - Abdallah et al. proposed the initial probabilistic model. You made some nice modifications and contributions. I propose we make both models available to the public (open source, open access), in order for further future improvements be made by others.

A. The authors agree that this would be beneficial to the research community.

Figure 13 shows samples of perturbed C_l and C_d curves. I notice that the C_l perturbations for positive angles of attack are shown but not for the negative angles of attack. Does this mean that the model does not handle C_l perturbations for negative angles of attack? If not it should, especially that you consider ultimate loads and large yaw errors.

A. Analysis was intentionally limited to only consider normal range of operation. As such, the C_l perturbations were limited to the range between the beginning of the linear C_l region and 90° . The beginning of the linear region is found to begin as low as $\alpha = -13^\circ$.

It is not clear if you maintain the correlations of C_l and C_d curves along the span of the blade?

A. The perturbations are made at the blade tip and root and interpolated to the airfoil data between these extremes.

Control properties, Table 10 - -20 to 20 degrees is a fairly large range for standard yaw error for a turbine in normal operation and connected to the grid, which might explain why this parameter ends up being so significant as shown in Figure 13, 14, and Table 11. Unless the underlying assumption is that this range implicitly includes the effect of rapid directional change of the wind. In principle a controller should be able to detect such large yaw errors (say over a 30-60 second averaging windows) and perform the necessary safety procedure (whatever that might be).

A. This is the value found in the literature and seems reasonable given the authors' discussions with experts.

Figure 13 has the grid on, Figure 14 has the grid off.

A. This has been fixed.

Page 25, Line 13: "Ultimate turbine loads are most sensitive to yaw error (θ) and lift (C_l) distribution" I would say "Both Ultimate and fatigue loads are..."

A. As fatigue loads are not most sensitive to the lift distribution, this adjusted statement would be incorrect.

Page 27, Lines 3-17: very good discussion. Useful information here that needs to be carried out to future investigations!

A. Agreed.

Page 35, Line 8-10: very good discussion. Useful information here that needs to be carried out to future investigations!

A. Agreed.

REVIEWER 2

1 General comments

1.1 Summary of key points

The paper is well written and its topic is relevant. The goals are clearly stated: sensitivity analyses for the NREL 5 MW turbine. They are ambitious because a large number of input and output variables are involved and a computationally demanding model (OpenFAST-based) is used. The choice to reduce the complexity of the analysis by using the relatively simple Elementary Effects approach is judicious. However, it seems to me that nevertheless, the problem is still too complex. To be able to tackle it, the authors work with a relatively small set of input vectors. This is the main weakness I find to be present in their analysis and they have not convincingly argued that the number of input vectors is sufficient.

A. The authors parameterized inflow inputs based on the capabilities of TurbSim and parameterized the turbine inputs to represent the main physical effects where uncertainties were probable.

A further issue is their adaptation of the Elementary Effects approach in a way that is insufficiently justified. The current exposition leaves me doubting that it is really a consistent sensitivity analysis approach. This does not mean that all their conclusions are arbitrary. On the contrary, I would guess that many conclusions about sensitivities are correct due to their broadly consistent nature over the whole input space and remain unaffected by details of the sensitivity analysis. (This may mean that they would also appear in simpler analyses and could perhaps be obtained from expert elicitation.)

A. Elementary Effects at its fundamental level can only be considered a screening method. However, the introduction of the use of Sobol numbers and radial trajectories increases its efficacy as a method for estimating sensitivity, not just as a screening method. Campolongo empirically demonstrated that the results obtained by EE can converge to a variance-based sensitivity index with increased number of Sobol points. In this work, the authors increased the number of Sobol starting points until the EE-based sensitivity metrics had shown convergence.

Despite my rather negative judgment about the method and assumptions, there are some gems in this paper. Notably, the authors' efforts in obtaining useful ranges for input variables have resulted in overview tables that are more broadly useful in their own right.

A. Agreed.

1.2 Overview of review aspects

My judgments here are based on my current understanding of the work. Brief justifications are given, but detail and nuance for the negative comments are postponed to the 'Specific comments' section. They may change due to clarification by author comments.

1. Does the paper address relevant scientific questions within the scope of WES?

Yes. Knowledge about sensitivities is of great value to wind turbine design and selection.

2. Does the paper present novel concepts, ideas, tools, or data?

Some. Novel variants of Elementary Effects sensitivity analysis are presented. A lot of interesting, new simulation data was generated and used.

3. Is the paper of broad international interest?

Yes. The discussion is relevant for all locations and in various wind energy research subdomains.

4. Are clear objectives and/or hypotheses put forward?

Yes. To provide sensitivities of relevant output variables relative to coherent sets

of input variables.

5. Are the scientific methods valid and clear outlined to be reproduced?

Validity may be tenuous and reproduction would be difficult. (i) I have my doubts that the novel variants of Elementary Effects sensitivity analysis is a proper sensitivity analysis.

A. See above discussion.

(ii) The determination of input variables is not discussed in sufficient detail for them to be even approximately recreated.

A. All input parameter ranges are referenced where possible. The authors believe this to be sufficient.

6. Are analyses and assumptions valid?

One important one is not. I find it doubtful that the set of input vectors is large enough to warrant conclusions as concrete as the ones drawn, even more so given that a nontrivial number of them may not correspond to physical situations.

A. The authors attempted to select turbine input parameters that are independent from each other. To minimize correlations to inflow input parameters, the results were binned by mean wind speed.

7. Are the presented results sufficient to support the interpretations and associated discussion?

No. This is a consequence of my evaluation of the two preceding points.

A. The authors have addressed these points.

8. Is the discussion relevant and backed up?

Yes. Based on the results the authors present, the conclusions are reasonable.

9. Are accurate conclusions reached based on the presented results and discussion?

Ambiguous. Given the presented results and discussion, the conclusions are accurate, but I think that flaws in the analysis and assumptions cast doubt on that accuracy.

A. These concerns have been addressed above.

10. Do the authors give proper credit to related and relevant work and clearly indicate their own original contribution?

Yes. According to my knowledge they certainly do. And notably, they make very good use of information in the literature for ranges of input variable values.

11. Does the title clearly reflect the contents of the paper and is it informative?

It can be improved. Currently, the title implies a scope that is larger than in actuality and is a bit long and complex. Suggestion: "Elementary effects sensitivity analyses of the NREL 5 MW turbine"

A. The title has been modified.

12. Does the abstract provide a concise and complete summary, including quantitative results?

Yes, but. (i) Quantitative results are not given, but neither are they appropriate. (ii) The future applications listed are not sufficiently discussed in the paper to be included.

A. The future applications provide the justification for doing the research in the paper and are therefore included in the abstract.

13. Is the overall presentation well structured?

Yes.

14. Is the paper written concisely and to the point?

Yes. There is a bit of repetition in the presentation of the second case study, but this redundancy may actually make the paper easier to read.

15. Is the language fluent, precise, and grammatically correct?

Yes.

16. Are the figures and tables useful and all necessary?

Not all. I found Figures 5–8, 10–11, and 15–22 of limited usefulness; the information should be more filtered and summarized to be useful. In contrast to these stand especially Figures 9 and 23.

A. Some figures have been moved into an appendix.

17. Are mathematical formulae, symbols, abbreviations, and units correctly defined and used according to the author guidelines?

Not all or in all aspects. Standards about notation of variables and constants are not followed and a mixture of fonts is distractingly used for mathematical notation.

A. The authors have attempted to improve on this. Additionally, the paper will go through a formal review process with an editor. Any remaining issues will be addressed at that time.

18. Should any parts of the paper (text, formulae, figures, tables) be clarified, reduced, combined, or eliminated?

Yes. For example, Figures 5–8, 10–11, and 15–22 as mentioned above.

A. Some plots have been moved to the appendix.

19. Are the number and quality of references appropriate?

Yes.

20. Is the amount and quality of supplementary material appropriate and of added value?

No supplementary material has been provided. It would have been useful if the simulation data (inputs, outputs) were made available, but it is of course the prerogative of the authors not to do so.

A. The authors believe that this is impractical, especially for an already lengthy paper.

2 Specific comments

2.1 Your modified EE formulae

There is insufficient justification of your modified formulae. You indicate why you add Y_{ob} in Eq. (3) and use a dimensional version, but just mentioning it is insufficient as an explanation. To me, adding a constant term to a set of sensitivities will substantially distort the information present in the quantity; it is not a sensitivity anymore. I can sense a reason for making it dimensional, but I can think of other reasons why this is a bad idea; you should pre-emptively remove such doubts. Currently, I am not convinced at all that what you call a sensitivity here can be interpreted and used as such.

A. The inclusion of Y_{ob} was necessary to properly compare ultimate load consistently across the bins because it is only the maximum ultimate load that matters.

In Eq. (5), you multiply by a probability and again indicate why, but do not explain it at all. Here, I can guess at the reason. Part of my reticence here is due to the fact that I am skeptical of your approach to the identification of most sensitive inputs; this is discussed next. As your modifications here are, I assume, related to your non-standard approach, it may be good to explain them concurrently in the text.

A. The scaling by the probability was necessary to properly compare fatigue loads consistently across the bins because it is the cumulative effect of all bins that matters for fatigue.

2.2 Your approach to the identification of most sensitive inputs

First of all, by looking at plain means, you implicitly assume that your samples are uniformly distributed over the input space. Even if you cannot justify this, you should at least discuss the implications. Related to this, you apparently do not calculate the expectation over wind speeds. Of course, for fatigue loads this is actually what happens because you have included the probability in the EE value. For ultimate loads, it does not, where I see no reason why you should throw away the probability information that you do have here and replace it with a uniform distribution (implicit by taking the plain mean, as said before).

A. The authors looked at the convergence of the number of starting points. Starting points were added until adding points no longer changed the mean of the EE values. Therefore, while there may be improbable events included in the parameter space, they do not affect the overall conclusions.

Second, you say that you do not use the standard approach, but do not really justify that. You refer to an appendix and there is information about that there, but take into account that appendices are meant for skippable material. When reading your approach and the standard one as sketched in the appendix, the latter was more appealing to me. The reason is that there the rankings are primarily based on the means.

A. The authors found that the exceedance approach was more justifiable and intuitive for the purpose of this research. The standard approach results was included in the appendix for potential readers who are interested in such results, but were not found to be the most beneficial presentation of this research.

You base your rankings essentially on tail behavior of the EE value distribution. Tail behavior says very little about what happens in the bulk of the distribution. It may well be that a distribution with a low mean but a fat tail generates more instances above your somewhat arbitrarily defined threshold than a distribution with a high mean but a skinny tail. Based on this reasoning, I fear that your approach may unduly rank higher inputs that generate fat tails, based just on the tail and not on the mean. It is possible that the tail behavior is similar over the inputs and then your criterion will work, but you do not show or discuss that. Even in that case I see no reason not to focus more on the means. So, a good start to convincing me is to explain why a ranking of means is not appropriate here and how your criterion overcomes the problems apparently present in other approaches.

A. The authors believe that the exceedance probability plots and histograms show such behavior and therefore allow for such concerns to be addressed in the analysis.

2.3 Your selection of input vectors

You use thirty input vectors times three—one for each wind speed bin—for both case studies. The quality of the selection of these points is essential, but the way in which you choose them is dealt with only in a single sentence where you claim that by using Sobol numbers—without providing details—you can ensure a wide sampling of the input hyperspace. Furthermore, you choose to ignore the dependencies between the input variables, but directly sample from the Cartesian product of the individual ranges you have defined, so non-physical input vectors could be included. Finally, your input spaces are very large, 18-dimensional and 40-dimensional respectively.

A. As mentioned above, a convergence study on the number of starting points was performed and the authors attempted to minimize correlations between inputs.

In such high-dimensional spaces, even a few dependencies can cause the subset of physical vectors to be 'small' relative to the Cartesian product. So it may be difficult to actually land on a physical vector, when those dependencies are not taken into account. (I do not see how using Sobol numbers can help with this issue, as more even sampling cannot correct for ignored dependencies.) This may mean that I cannot exclude the possibility that the majority or even all of the input vectors you use is non-physical. The fact that 90 input vectors in such high-dimensional spaces is a very small sample, only makes this issue more problematic. (I understand that for computational time reasons you cannot increase this number by orders of magnitude.) Because a priori I must assume that non-physical input vectors may result in non-realistic output sensitivities, this issue undermines your results.

In the conclusion, you state that "The combinations of parameters in this study spanned the ranges of several different locations." Given the reasoning I developed above, you will understand that I am skeptical of this. But this can be tested: how representative are your input vectors of existing locations? This may provide an avenue to reduce my worries about your selection of input vectors.

A. These concerns have been addressed above.

2.4 Your presentation of applications and future work

In the conclusions, you present a number of possible applications of your work and also ideas for future work. I feel that some—about error bars and insight—are described too briefly or too vague to really know whether indeed, your results provide a useful starting point.

A. The authors believe it is important to focus on what was done in the paper. Since this resulted in a lengthy paper, it was decided to simply highlight potential future work to save space.

3 Technical corrections

3.1 General

• In mathematical notation, the following standard conventions are prescribed: variables are written in a cursive/italic/slanted font and constants are written in a roman/upright font. <https://www.nist.gov/pml/nist-guide-si-chapter-10-more-printing-and-using-symbols-and-numbers-scientific-and-technical#102> Please do so throughout, as currently this is not adhered to and most every symbol is put in italic font, even word abbreviations (which are certainly constant).

A. The paper will go through a formal review process with an editor. Any remaining issues will be addressed at that time.

• As per the SI standards, between a value and a unit there should always be a normal (unbreakable) space. So do not write ‘5-MW’, but ‘5 MW’; there are other examples in the text where no space is present. Also, composed units should not be separated by a hyphen, use a centered dot instead; e.g., ‘kN·m’ instead of ‘kN-m’.

A. These corrections have been made throughout the paper.

• You abuse the same symbol for functions and variables: for example Y and Y_0 instead of f and f_0 ; avoid that, as it causes confusion.

A. The paper will go through a formal review process with an editor. Any remaining issues will be addressed at that time.

• Your presentation of the EE approach is symbolically far more verbose than it needs to be. Suggestions:

–Make effective use of vectorial notation. For example, Eq. (2) could be written as

$$E_i = f(-U + \Delta_{ci}) - f(-U)\Delta.$$

(Arrows instead of bold here only because of reviewing system limitations.)

A. This has been somewhat addressed. The paper will go through a formal review process with an editor. Any remaining issues will be addressed at that time.

–Use consistent notation for elements (lower case) and sets (upper case). For example $u \in U$, y instead of Y .

A. This has been somewhat addressed. The paper will go through a formal review process with an editor. Any remaining issues will be addressed at that time.

–Make subscripts more ‘direct’ by avoiding index layers and using variables directly. For example, v instead of both b and vb , u instead of both r and ur .

A. This has been somewhat addressed. The paper will go through a formal review process with an editor. Any remaining issues will be addressed at that time.

–Put commas between subscripts and do not overburden subscript/superscript locations.

A. This has been somewhat addressed. The paper will go through a formal review process with an editor. Any remaining issues will be addressed at that time.

–Predefine some recurring fragments, such as $\Delta v_i = \max U v_i - \min U v_i$ and $\delta v_i = \Delta v_i / 10$.

A. This has been somewhat addressed. The paper will go through a formal review process with an editor. Any remaining issues will be addressed at that time.

Combined, you could write Eq. (3), (4), and (5) as

$$\begin{aligned} EE_{vi,o}(\sim uv) &= \bar{y}_{vo} + 10|f_o(\sim uv \pm \delta v_i - c_i) - f_o(\sim uv)| \\ &\text{with } f_o(\sim uv) = 1|S|\sum_s \in S \max_t |f_o, s(\sim uv, t)|, \\ EE_{vi,o}(\sim uv) &= 10|g_o(\sim uv \pm \delta v_i - c_i) - g_o(\sim uv)|p(v) \\ &\text{with } g_o(\sim uv) = \dots \end{aligned}$$

A. This has been somewhat addressed. The paper will go through a formal review process with an editor. Any remaining issues will be addressed at that time.

• You use ‘parameters’ where I would use ‘variables’, given that the focus is on varying those quantities. For example, in your setup, I would call wind speed a variable, as it parameterizes some sub-cases, but is not varied as, e.g. wind shear is.

A. The authors chose to use “parameters” because that is the term used to define inputs in the aero-elastic software used in this research and makes the most sense in the context of this work.

• Throughout the paper, the formulation of sensitivities are according to my ear often reversed. In the paper, input variables are called ‘(most) sensitive’, whereas I would apply such language to output variables only. For input variables, words like ‘impactful’ and ‘influencing’ come to mind, although these do not seem ideal. Consider changing the language, but for the input side feel free to find a better word than the ones I came up with.

A. The authors prefer to keep the language as is, which has precedent in related publications.

• Do not break tables over multiple pages; if you must, repeat the header row.

A. This is absolutely true. However, as formatting will change significantly with final publication, this has not been specifically addressed here.

3.2 Local

p.2, 1.33 OpenFAST is software, not an approach.

A. This has been changed in the text.

p.3, 1.6 What does ‘down-selected’ mean?

A. This has been changed to “selected”.

p.3, 1.13 You must say how this was assessed.

A. This is thoroughly addressed in Section 3.

p.4, Table 1 This nice table can be improved by adding symbols and a clear indication of which variables are used for which case study (wind vs. turbine and ultimate vs. fatigue).

A. The authors believe that the table is best presented as is. All QoIs are used for all the studies.

p.4, §3.1 Paragraph way too long; split in two or three.

A. The paper will go through a formal review process with an editor. Any remaining issues will be addressed at that time.

p.5, 1.20 Elaborate, the current explanation about the ‘radial approach’ is too limited.

A. More explanation was provided in the paper.

p.5, 1.22 Elaborate, the current explanation is too limited. How did you obtain the Sobol numbers and how did you use them.

A. One can use Sobol sequences to fill up a space with "random" points. The nice thing about it is that the points distribute themselves fairly evenly and therefore sample the space uniformly (to a good extent) without having a pattern per se.

p.6, l.1 Say how and why it was modified or at least reference forward.

A. A reference note was made in the paper.

p.6, l.8 'nondimensionalizing' to 'making dimensionless/adimensional'

A. This change has been made.

p.6, l.9 'derivative' to 'finite difference'

A. This change has been made.

p.6, l.10 'IEC turbine class I and category B' to 'IEC turbine class I and category B' (to avoid confusion with index sets I and B)

A. This change has been made.

p.6, Eq. (3) and (5) $ib \pm 1$ to $bi \pm 1$ (but better still follow my general suggestions regarding math notation to avoid making such mistakes)

A. The paper will go through a formal review process with an editor. Issues such as this will be addressed at that time.

p.6, Eq. (4) In principle, the LHS depends on the set of seeds

A. The authors performed a convergence study on the number of seeds used in the study to ensure that the solution converged independent of the seeds.

p.6, l.20 Why choose the sign randomly? Does this matter?

A. This allowed for more of the multi-dimensional input parameter space to be considered.

p.6, l.20 and elsewhere 'IEC-Class IB' to 'IEC Class IB'

A. This change has been made throughout the text.

p.6, l.20 move 'The added term . . . ' forward in section.

A. This section has been rewritten.

p.6, l.23 Define DEL (as you should all letter words); do not assume all your readers will be familiar with this.

A. This term was previously defined on page 3, line 22.

p.7, l.6 Your notation includes indices that are in fact averaged away (r , i , b) for the mean EE value, but for the (sample) standard deviation, you include not even the one that isn't gone (o). Some consistent, standard notation would be appropriate here; consider something like the sample mean m_o and sample standard deviation s_o , perhaps.

A. The authors believe that once EE has been clearly defined, it is acceptable to simply state that the EE values have a mean and standard deviation.

p.7, l.8 The part about 'stratification' requires more explanation, certainly because it is not immediately clear in what way this differs between the two case studies. (Perhaps you can reference to a relevant earlier part of the text.)

A. This has been clarified.

p.7, l.8–12 The way in which you decide to include or exclude some wind speed bins comes across as somewhat arbitrary here. More explanation may be needed.

A. This section has been clarified.

p.7, l.17 'speed bins' to 'speeds'

A. The paper will go through a formal review process with an editor. Issues such as this will be addressed at that time.

p.7, 1.24 'Holtstag' to 'Holtslag'

A. This has been corrected.

p.7, 1.35 'either better optimized or lower risk': optimized for what? lower risk of what? Avoid vagueness here, as concrete applications are a good justification for your work.

A. By increasing accuracy, you are eliminating uncertainty in your analysis. A system would be better optimized if, based on reducing uncertainty, you are able to narrow your design margin. However, if your uncertainty was actually allowing you to have a design that had a higher probability of failure than expected, lowering this uncertainty would therefore reduce the risk of failure, as the system would be appropriately re-designed.

p.8, Table 2 use the same, correct mathematical symbol, e.g., ' $u(\sigma u)$ '.

A. This nomenclature is consistent with the IEC wind turbine design standard.

p.8, 1.16 Suggestion: for q, use the velocity component name directly, instead of an index.

A. The paper will go through a formal review process with an editor. Issues such as this will be addressed at that time.

p.8, 1.19–21 Giving the exact quantity definitions of the IEC standard here is superfluous, certainly because you do not use it.

A. The authors believe these definitions are important in the context of this work.

p.8, 1.22 'and random' to 'and to the random' (?)

A. The authors believe the grammar is fine as is.

p.9, 1.9–10 'term' to 'factor'

A. This has been corrected.

p.9, 1.11 'in (IEC, 2005)' to 'in the standard (IEC, 2005)' (text should make sense when reading aloud, skipping over citation parentheticals)

A. This has been corrected.

p.9, 1.30 'B' to 'B'

A. This has been corrected.

p.10, Table 3 header

• There is no need for parentheses around units.

A. The authors disagree. This is standard practice.

•bu,bv,bw are not dimensionless; I suggest using 1/mm for convenient notation of the values.

A. This has been corrected.

p.10, Table 3 footnote Elaborate a bit.

A. At extremely negative values of the shear exponent, α , tower blade strikes would often occur. To eliminate this issue, the minimum value of α was changed to -0.75 from -1.5.

p.10, 1.7 'unphysical' to 'non-physical'

A. This has been corrected.

p.11, Fig. 3–4 Suggestion: use a logarithmic axis for the counts, then zooming will not be necessary and more information should become visible.

A. The authors originally used a logarithmic scale on the y-axis. However, it was found that the figures are easier to interpret without a logarithmic axis.

p.19, Tables 4–5 Make it explicit in the table whether the numbers given are percentages or counts.

A. This has been clarified in Tables 4, 5, 12, and 13.

p.20, 1.8–9 Provide more information about the expert(s) and the elicitation procedure used.

A. When references were not available for specific parameters, experts in the area of study at the NWTC were sought out.

p.20, Table 6• Do not use the empty set symbol \emptyset instead of the Greek letter phi ϕ .

A. This has been corrected.

•BM,imb to BM,imb (just an example of the type of math font use corrections that you should implement; note that the font of the subscripts, which here refer to words, are upright)

A. These corrections have been made throughout the paper.

p.21–22, list around page break What are the parenthetical, bold math symbols for?

A. They are identifying the symbols that are associated with the described parameters.

p.22, Figure 12 Avoid putting figures in the middle of paragraphs.

A. This is something that will be changed with final formatting. As such, it is not addressed here.

p.23, 1.18–19 Avoid line breaking tuples.

A. Again, this will be changed in final formatting and is not addressed here.

p.23, 1.19–20 Use paragraph breaks as defined by the style.

A. Again, this will be changed in final formatting and is not addressed here.

p.24, Figure 13 •Are curves for Cd,orig and Cd,-10% missing here, or do they just overlap?

A. The lines overlap. This is explained in the text.

• This Figure is not referenced in the text, I think. (All figures and tables should be.)

A. This reference was accidentally deleted during formatting and has been added back in on page 23, line 17.

p.25, 1.8–23 This paragraph is too long; split.

A. While the paragraph might be lengthy, the authors believe that all of this information belongs in one paragraph.

p.25, 1.17 'relevant' to 'relative' (?)

A. This change has been made.

p.27, 1.3–17 This paragraph is too long; split.

A. While the paragraph might be lengthy, the authors believe that all of this information belongs in one paragraph.

p.37, 1.1 'hear' to 'here'

A. This has been corrected.

p.38, Figures 24–25 I think that plots of σ/μ vs. μ would provide more insight here.

A. Plots of σ vs μ are standard practice in EE literature. Since these plots were included to show the results in the standard way, they are kept as is.

REVIEWER 3

Very interesting paper with very interesting and useful results. The baseline methodology should be described in more detail in order to stand out as reference. For other wind systems. In particular sections 3.3.1 and 3.3.2 should be revised to clarify to the reader in which way the initial function was adjusted. This is done good on a detailed level, but it would help to get a higher-level summary of the idea behind the applied procedure.

A. Yb was necessary to properly compare ultimate load consistently across the bins because it is only the maximum ultimate load that matters. The scaling by the probability was necessary to properly compare fatigue loads consistently across the bins because it is the cumulative effect of all bins that matters for fatigue.

Also, it should be highlighted throughout the paper that the approach is a tailored approach for the problem at hand. The alteration of the baseline formulas as well as the threshold evaluation of EE indicates that classical SA is not applied. There are good reasons presented for it, and i expect the results to be valid nonetheless, but the variation of standard approaches is significant.

A. Some language was added to the paper to address this comment.

The plots are quite comprehensive. It could be sufficient to just show exemplary plots to describe the applied methodology, and provide the full set of plots inside the appendix. The summarizing tables are very helpful.

A. Some plots have been moved to the appendix.

EE is generally used as screening method, in order to identify relevant input parameters. In this sense, the values of the resulting EE should be handled with care. They only provide an indicator of relevance, not of the sensitivity (or even the comparative relevance). This should be taken into account when evaluating the resulting EEs.

A. Elementary Effects at its fundamental level can only be considered a screening method. However, the introduction of the use of Sobol numbers and radial trajectories increases its efficacy as a method for estimating sensitivity, not just as a screening method. Campolongo empirically demonstrated that the results obtained by EE can converge to a variance-based sensitivity index with increased number of Sobol points. In this work, the authors increased the number of Sobol starting points until the EE-based sensitivity metrics had shown convergence.

Page 1: "sensitive" to "influential:

A. The authors believe that "sensitive" is the proper term in this case.

Page 1: are you sure? to my knowledge, EE is not suitable for the quantification of uncertainty..

A. See explanation above.

Page 2: towards

A. Due to the placement of this comment in the document, the authors are unsure what it is referring to.

Page 2: not 100% sure since no native english speaker myself, but shouldnt it be the "sensitivity of an output towards an input" rather than the other way around? in the same way i would write here "impact of input on response,..."

A. I have changed it to "sensitivity due to each input"

Page 2: so different number of seeds for each design point? what was the employed convergence threshold?

A. The same number of seeds was used for each design point. To establish a convergence threshold, the authors visually examined the convergence to ensure that differences between the EE values across the design points were larger than differences between seeds.

Page 3: somewhat out of touch with the motivation of EE, which is screening.

A. This comment is in relation to the fact that we had to first choose a set of parameters for the study, which involved down-selecting from a large list of possible ones. If all parameters would be considered, the total number could reach into the thousands. The approach used here was to choose those that spanned the characteristics being considered, and in a succinct manner. For instance, the TurbSim model parameters were chosen as an effective representation of the parameters for wind-inflow characterization.

Page 3: this figure is very high level and does not contain a lot of information, but does take a lot of space. consider leaving out?

A. The authors believe that this figure aids in the explanation on the setup and considered parameters.

Page 3: i think in sensitivity terminology this would be the dependent or output parameters. it might be valuable to stick to the same nomenclature in order to avoid confusion?

A. The authors have changed the text to consistently use "QoI" throughout the text.

Page 3: vector sum based on the time series or on the ULS results of the time series?

A. The vector sum was taken at each time step.

Page 4: in table 1

A. This sentence is referring to the processes of used to assess the sensitivity of the input parameters, which is separate from the QoIs described in Table 1. This has been clarified in the text.

Page 4: not sure if this is correct ("common")

A. The authors believe this is correct.

Page 4: including meta modeling

A. We are unsure of the meaning of this comment. The sentence is about meta modeling.

Page 4: dont understand this comparison. the choice of sensitivity analysis is more or less independent from the choice of sampling procedure..

A. The discussion here is on how to improve the time efficiency of a sensitivity analysis. This can be done either through the mathematical approach for calculating the sensitivity, or through a down-selection of simulations based on the important ones, or through a reduced-order model.

Page 4: elementary effect

A. I'm assuming that the reviewer would like us to spell out EE here? The name has been introduced before, as well as the acronym, but we will go ahead and spell it out again here.

Page 5: R is 10 in this work => 10%?
how is this value selected?

A. R is 30 in this work and was selected based on a convergence study that considered all QoIs.

Page 5: in line with proposed method from campolongo, no? should be sufficient to only highlight the differences from there

A. Campolongo has looked at multiple approaches, so the authors thought it would be useful to provide a high-level summary of the approach being taken.

Page 5: reference?

A. A reference has been added.

Page 6: clarify again that i is for the input variables

A. The authors do not believe this is necessary, as the parameter is defined multiple times before this point.

Page 6: r is iterating from 1 to 10?

A. 30 starting points are used in this work. r is not necessarily iterating from 1 to 30, but is instead being calculated separately at each starting point.

Page 7: difficult statement. EE already describes the sensitivity. Do you have an "exact" sensitivity in mind that is modeled with the EE?

A. There is a sensitivity formula suggested by Campolongo, and introduced by Janson. In the end, the formula is very similar to the μ^* metric associated with Elementary Effects, and is therefore used directly as a sensitivity metric.

Page 7: can you explain your motivation of deviating from the classical procedure? is this resulting from introducing new measures of EE which deviates from general methodology?

A. The classical method has a pictorial representation of mean vs standard deviation of the EE values. There is no definitive procedure for identifying or selecting the most significant parameters. The metric devised here is focused only on μ^* (mean) as this is the sensitivity indicator, whereas the standard deviation is an indicator of the influence of other parameters.

Page 7: is there a general procedure on how to assess these thresholds?

A. The authors chose a value that was reasonable given the data.

Page 7: also an interesting paper from Kelly and Dimitrov using pce to establish Sobol indices

A. Thank you for the additional reference. However, since this was not used when establishing the method we did not add it as a reference in the paper.

Page 8: should be highlighted in the abstract that a kaimal spectrum was used

A. A statement has been added to the abstract.

Page 11: you show results across all QoI, right?

A. Correct. These results are presented in Figures 5-8 and Figures 15-18.

Page 24: this seems very large

A. The level of yaw error was based on a reference by Quick, and the author's agreed that this level was feasible by consulting experts.

Page 27: should be mentioned in section on methodology or outlook as well

A. The general methodology is summarized above. There were issues encountered for this second case study, and we felt it was best to discuss the issues encountered within the individual study, since they did not occur for the other case study.

Page 27: this paragraph should be revised to increase readability.

A. The paper will go through a formal review process with an editor. This will be addressed at that time.

Page 36: the purpose of EE is more the determination of relevant input parameters, not the sensitivity assessment. This should not be the motivation of this study.

A. Please see discussion above.

Page 36: is there any improvement possible on the applied procedure in this work for other systems or do you propose that it can be used as a baseline method?

A. Though minor adjustments may need to be made, the overall process is quite applicable to the related analyses.

Sensitivity of Uncertainty Sensitivity Analysis of Wind Characteristics and Wind Turbine Properties on Wind Turbine Extreme and Fatigue Loads

Amy N. Robertson¹, Kelsey Shaler¹, Latha Sethuraman¹, Jason Jonkman¹

¹National Renewable Energy Laboratory, 15013 Denver West Parkway, Golden, CO 80401, USA

Correspondence to: Amy N. Robertson (amy.robertson@nrel.gov)

Abstract. Wind turbine design relies on the ability to accurately predict turbine ultimate and fatigue loads. The loads analysis process requires precise knowledge of the expected wind-inflow conditions as well as turbine structural and aerodynamic properties. However, uncertainty in most parameters is inevitable. It is therefore important to understand the impact such uncertainties have on the resulting loads. The goal of this work is to assess which input parameters have the greatest influence on turbine power, fatigue loads, and ultimate loads during normal turbine operation. An Elementary Effects (EE) sensitivity analysis is performed to identify the most sensitive parameters. Separate case studies are performed on 1) wind-inflow conditions and 2) turbine structural and aerodynamic properties, both using the National Renewable Energy Laboratory (NREL) 5-MW-5-MW baseline wind turbine. The Veers model was used to generate synthetic IEC Kaimal turbulence spectrum inflow. The focus is on individual parameter sensitivity, though interactions between parameters are considered.

The results of this work show that for wind-inflow conditions, turbulence in the primary wind direction and shear are the most sensitivity parameters for turbine loads, which is expected. Secondary parameters of importance are veer, u-direction integral length, and components of the IEC coherence model (σ_u and σ_v), as well as the exponent (α). For the turbine properties, the most sensitive parameters are yaw misalignment (θ) and outboard lift coefficient ($C_{L,OB}$) distribution. This information can be used to help establish error bars around the predictions of engineering models during validation efforts, and provide insight to probabilistic design methods and site-suitability analyses.

1 Introduction

Wind turbines are designed using the IEC 61400-1 standard, which prescribes a set of simulations to ascertain the ultimate and fatigue loads that the turbine could encounter under a variety of environmental and operational conditions. The standard applies safety margins to account for the uncertainty in the process, which comes from the procedure used to calculate the loads (involving only a small fraction of the entire lifetime), but also from uncertainty in the properties of the system, variations in the conditions the turbine will encounter from the prescribed values, and modeling uncertainty. As manufacturers move to develop more advanced wind technology, better optimized designs, and reduce the cost of wind turbines, it is important to better understand how uncertainties impact modeling predictions and reduce the uncertainties where possible. Knowledge of where the uncertainties stem from can lead to a better understanding of the cost impacts and design needs of different sites and different turbines.

This paper provides a better understanding of the uncertainty in the ultimate and extreme structural loads and power in a wind turbine. This is done by parameterizing the uncertainty sources; prescribing a procedure to estimate the load sensitivity to each parameter; and identifying which parameters have the largest sensitivities for a conventional utility-scale wind turbine under normal operation. An Elementary Effects methodology was employed for estimating the sensitivity of the parameters. This approach was chosen as it provides a reasonable estimate of sensitivity, but with significantly less computational requirements

Formatted: Font: (Default) Times New Roman

Formatted: Font: 10 pt

Formatted: Font: Not Italic

Formatted: Font: Not Italic

Formatted: Font: Not Italic

Formatted: Font color: Auto

Formatted: Font color: Auto

compared to calculating the Sobol sensitivity, and without increasing the uncertainty in the result through the use of a reduced-order model. Some modifications were needed to the standard Elementary Effects approach to properly compare loads across different wind speed bins.

5 This work is a first step in understanding potential design process modifications to move towards a more probabilistic approach or to inform site-suitability analyses. The results of this work can be used to 1) rank the sensitivities of different parameters, 2) help establish error bars around the predictions of engineering models during validation efforts, and 3) provide insight to probabilistic design methods.

2 Analysis Approach

10 2.1 Overview

To identify the most influential sources of uncertainty in the calculation of the structural loads for utility-scale wind turbines, a sensitivity analysis methodology based on Elementary Effects (EE) is employed. The focus is on the sensitivity of the input parameters of wind turbine simulations (used to calculate the loads), not on the modeling approach-software itself, which creates uncertainty based on whether the approach used accurately represents the physics of the wind loading and structural response. The procedure followed is summarized in the following sub-sections. The caveats of the sensitivity analysis approach employed are given as follows:

- Only the NREL 5-MW5-MW reference turbine is used to assess sensitivity (the resulting identification of most-sensitive parameters may depend on the turbine).
- Only normal operation under turbulence is considered (gusts, start-ups, shut-downs, and parked/idling events are not considered).
- Min/max values of the input parameter uncertainty ranges are examined in the analysis (no joint probability density function is considered).
- With the exception of wind speed, each parameter is examined independently across the full range of variation, and is not conditioned based on other parameters.

25 2.2 Wind turbine model and tools

The sensitivity due to each input parameter on turbine load response is assessed through the use of a simulation model. The NREL 5-MW5-MW reference turbine (Jonkman et al., 2009) was used in this study as a representative turbine. This is a variable-speed, 3-bladed, upwind, horizontal-axis turbine with a hub height of 90 m and a rotor diameter of 126 m. Though not covered in this work, it would also be useful to examine in future work how the sensitivity of the parameters on turbine loads is affected by the size and type of the considered wind turbine.

The effect of input parameters on load sensitivity could be influenced by the wind speed and associated wind turbine controller response. Therefore, the EE analysis was performed at three different wind speeds corresponding to mean hub height wind speeds of 8, 12, and 18 m/s, representing below-, near-, and above-rated wind speeds, respectively. Turbulent wind conditions were generated at each wind speed using TurbSim (Jonkman, 2009), employing an IEC Kaimal turbulence spectrum with exponential spatial coherence. Multiple turbulence seeds were used for each input parameter variation to ensure the variation from input parameter changes is distinguishable from the variation of the selected turbulence seed. The number of seeds was determined through a convergence study for each of the parameter sets. A 25 x 25 point square grid of three-component wind vector points that encompasses the turbine rotor plane was used.

OpenFAST, a state-of-the-art engineering-level aero-servo-elastic modeling approach, was used to simulate the NREL 5-MW5-MW wind turbine using the developed wind files, allowing for aeroelastic response and turbine operation analysis. A simulation time of 10 minutes was used after an initial 30-second transient period per turbulence seed. Drag on the tower was not considered because it is negligible for an operational turbine. AeroDyn, the aerodynamic module of OpenFAST, determines

the impact of the turbine wake using induction factors that are computed using blade-element momentum (BEM) theory with advanced corrections. Steady and unsteady aerodynamic response were considered. Steady aerodynamic modeling uses static lift and drag curves in the momentum balance to calculate the local induction. Unsteady airfoil aerodynamic modeling accounts for dynamic stall, flow separation, and flow reattachment to calculate the local aerodynamic applied loads. ElastoDyn, a combined multibody and modal structural approach that includes geometric nonlinearities, was used to represent the flexibility of the blades, drivetrain, and tower and compute structural loading, which was used to compute ultimate and fatigue loads. The baseline controller of the NREL 5-MW5-MW turbine was enabled using ServoDyn. OpenFAST results were used to assess the change in response quantities of interest (QoIs) to changes in the physical input parameters.

2.3 Case Studies

Input parameters were identified that could significantly influence the loading of a utility-scale wind turbine. These parameters were organized into two main categories (or case studies): the ambient wind-inflow conditions that will generate the aerodynamic loading on the wind turbine and the aeroelastic properties of the structure that will determine how the wind turbine will react to that loading (see Figure 1). Within these two categories, a vast number of uncertainty sources can be identified, and Abdallah (2015) provides an exhaustive list of the properties. For this study, the authors down-selected those parameters believed to have the largest effect for normal operation for a conventional utility-scale wind turbine, which are categorized into the labels shown in Figure 1.

To understand the sensitivity of a given parameter, a range over which that parameter may vary needed to be defined. For the wind conditions, a literature search was done to identify the reported range for each of the parameters across different potential wind-farm locations within the three wind speed bins. For the aeroelastic properties, the parameters are varied based on an assessed level of potential uncertainty associated with each parameter.

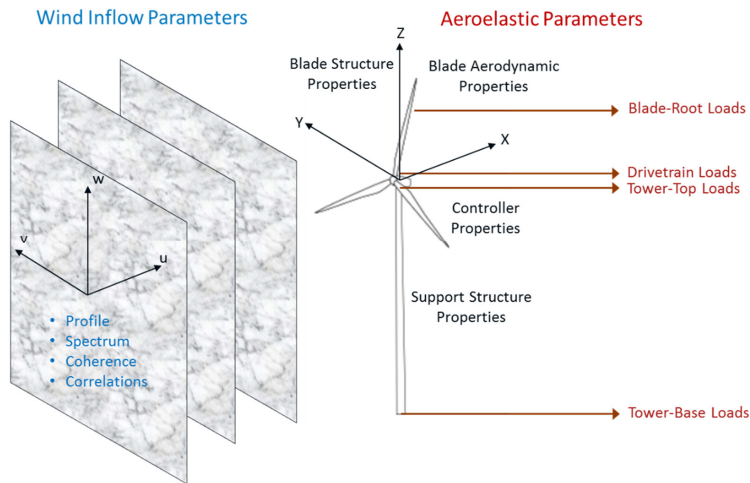


Figure 1: Overview of the parametric uncertainty in a wind turbine loads analysis. Includes wind-inflow conditions (subset shown in blue), turbine aeroelastic properties (subset shown in black), and the associated load QoI (subset shown in red).

2.4 Quantities of Interest

To capture the variability of turbine response that results from parameter variation, several QoIs were identified. These QoIs are summarized in Table 1 and include the blade, drivetrain, and tower loads; blade-tip displacement; and turbine power. Ultimate and fatigue loads were considered for all load QoIs, whereas only ultimate values were considered for blade-tip displacements. The ultimate loads were estimated using the average of the global absolute maximums across all turbulence seeds for a given set of parameter values. The fatigue loads were estimated using damage-equivalent loads (DEL) of the [output QoI](#) response across all seeds for a given set of parameter values. For the bending moments, the ultimate loads were calculated as the largest vector sum of the first two components listed, rather than considering each individually. The QoI sensitivity of each [input](#) parameter is examined using the procedure summarized in the next section.

Table 1. Quantities of interest examined in the sensitivity analyses.

| Quantity of Interest | Component | | |
|---|------------------------------|-------------------|-----------------|
| Blade-root moments | Out-of-plane bending | In-plane bending | Pitching moment |
| Low-speed shaft moments at main bearing | 0-degree bending | 90-degree bending | Shaft torque |
| Tower-top moment | Fore/aft bending | Side/side bending | Yaw moment |
| Tower-base moment | Fore/aft bending | Side/side bending | |
| Blade-tip displacement | Out-of-plane (Ultimate only) | | |
| Electrical power | | | |

3 Sensitivity Analysis Procedure

3.1 Sensitivity Analysis Approaches

There are many different approaches to assess the sensitivity of the QoI for a given input parameter. The best choice depends on the number of considered input parameters, simulation computation time, and availability of parameter distributions. Sensitivity is commonly assessed through the Sobol sensitivity (Saltelli et al., 2008), which decomposes the variance of the response into fractions that can be attributed to different input parameters and parameter interactions. The drawback of this method is the large computational expense, which requires a Monte Carlo analysis to calculate the sensitivity. To decrease the computational expense, one approach is to use a meta-model, which is a lower-order surrogate model trained on a subset of simulations to capture the trends of the full-order, more computationally expensive model. This approach has been used in the wind energy field (Nelson et al., 2003; Rinker, 2016; Sutherland, 2002; Ziegler et al., 2016), but was deemed unsuitable for this work given the wind turbine model complexity and associated QoIs. Specifically, it may be difficult for a meta-model to capture the system nonlinearities and interaction of the controller, especially the ultimate loads, limiting meta-model accuracy. Another approach to reduce computational expense is to use a design of experiments approach to identify the fewest simulations needed to capture the variance of the parameters and associated interactions, *e.g.*, Latin hypercube sampling (Matthaus et al., 2017; Saranyasontorn, 2006; Saranyasontorn et al., 2008) and fractional factorial analysis (Downey, 2006). These methods were considered for this application, but such approaches are still too computationally expensive given the large number of considered input parameters. Instead, a screening approach was determined to be the best approach. A screening method provides a sensitivity measure that is not a direct estimate of the variance, but rather supplies a ranking of those parameters with the most influence. One of the most commonly used screening approaches is called [Elementary Effect \(EE\)](#) analysis (Compolongo et al., 2007; Campolongo et al., 2011; Francos et al., 2003; Gan, 2014; Huang et al., 2012; Jansen, 1999; Martin et al., 2016; Saint-Geours et al., 2010; Soheir et al., 2015). Once the EE analysis identifies the input parameters that are most influential to the QoIs, a more targeted analysis can be performed using one of the other sensitivity analyses discussed above.

3.2 Overview of Elementary Effects

EE at its core is a simple methodology for screening parameters. It is based on the one-at-a-time approach in which each input parameter of interest is varied individually while holding all other parameters fixed. A derivative is then calculated based on the level of change in the QoI to the change in the input parameter using first-order finite differencing. Approaches such as these are called local sensitivity approaches because they calculate the influence of a single parameter without considering interaction with other parameters. However, the EE method extends this process by examining the change in response for a given input parameter at different locations (points) in the input parameter hyperspace. In other words, only one parameter is varied at a time, but this variation is performed multiple times using different values for the other input parameters, as shown in Figure 2. The derivatives calculated from the different points are considered to assess an overall level of sensitivity. Thus, the EE method considers the interactions between different parameters and is therefore considered a global sensitivity analysis method.

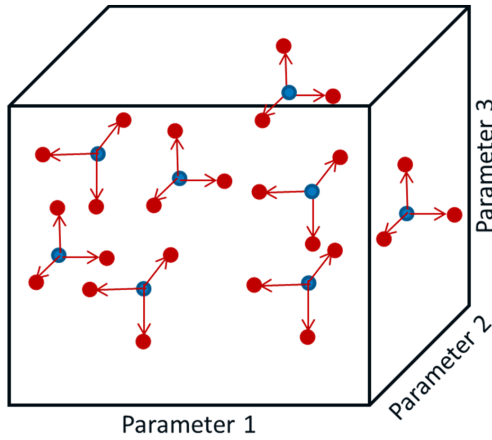


Figure 2: Radial EE approach representation for 3 input parameters. Blue circles indicate starting points in the parameter hyperspace. Red points indicate variation of one parameter at a time. Each variation is performed for 10% of the range over which the parameter may vary, either in the positive or negative direction.

Each wind turbine QoI, \underline{Y} , is represented as a function of different characteristics of the wind or model property input parameters, \underline{U} , as follows:

$$\underline{Y} = f(u\psi_1, \dots, u\psi_i, \dots, u\psi_I) \quad (1)$$

where I is the total number of input parameters. In the general EE approach, all input parameters are normalized between 0 (minimum value) and 1 (maximum value). For a given sampling of \underline{U} , the EE value of the input parameter, i , is found by varying only that parameter by a normalized amount, Δ :

$$EE_i = \frac{f(U+x_k) - f(U)}{\Delta} \quad (2)$$

where

$$x_k = \begin{cases} 0 & \text{for } k \neq i \\ \Delta & \text{for } k = i \end{cases} \quad (3)$$

Formatted: Font: Bold, Not Italic, Font color: Auto

Formatted: Font: Not Italic

Because of the normalization of \mathbf{U} , the elementary effect (EE) value (EE) can be thought of as the local partial derivative of the \mathbf{Y} with respect to an input (u_i), scaled by the range of that input. Thus, the EE value has the same unit as the output QoI. The EE value is calculated for R starting points in the input parameter hyperspace, creating a set of R different calculations of EE value for each input parameter.

Formatted: Font: Not Italic, Font color: Auto

The basic approach for performing an EE analysis has been modified over the years to ensure that the input hyperspace is being adequately sampled and to eliminate issues that might confound the sensitivity assessment. In this work, the following modifications to the standard approach were made:

1. A radial approach, where the EE values were calculated by varying each parameter one at a time from a starting point (see Figure 2), was used rather than the traditional trajectories for varying all of the parameters, which has been shown to improve the efficiency of the method (Campolongo et al., 2011).
2. Sobol numbers were used to determine the initial points at which the derivatives will be calculated (blue circles in Figure 2), which ensures a wide sampling of the input hyperspace (Campolongo et al., 2011; Robertson et al., 2018).
3. A set delta value equal to 10% of the input parameter range ($\Delta_{ib} = \pm 0.1 u_{ib,range}$) was used to ensure the calculation of the finite difference occurred over an appropriate range to better meet the assumption of linearity.
4. A modified EE formula—different for ultimate and fatigue loads—was used to examine the sensitivity of the parameters across multiple wind speed bins. EE modifications are detailed in (see Sections 3.3.1 and 3.3.2 for more information on the modifications).

3.3 Elementary Effects Formulas

This section provides the detailed formulas used to calculate the EE values for the ultimate and fatigue loads.

3.3.1 Ultimate Loads

When considering the ultimate loads, only the single highest ultimate load is of concern, regardless of the wind speed bin. Therefore, the standard EE formula is modified so that the sensitivity of the parameters can be examined consistently across different wind speed bins. This is accomplished by keeping \mathbf{U} and Δ dimensional (i.e., not making nondimensionalizing \mathbf{U} dimensionless between 0 and 1), multiplying the derivative, approximated with a finite difference, by the total range of the input for a given wind speed bin, and adding the nominal value of the QoI associated with IEC turbine class I and category B (IEC Class IB) for the given wind speed bin. The EE of input parameter U_{ib}^r for a certain QoI, \mathbf{Y} , at starting point r in wind speed bin b is then given by:

Formatted: Font: Not Italic

Formatted: Font: Not Italic

$$EE_{ib}^r = \left| \frac{Y(\mathbf{U}^r + \mathbf{x}_k) - Y(\mathbf{U}^r)}{\Delta_{ib}} u_{ib,range} \right| + \bar{Y}_b \quad (4)$$

where \bar{Y}_b represents the IEC Class IB nominal value for the given wind speed bin; and the ultimate load, $Y(\mathbf{U})$, is defined as the mean of the absolute maximum of the temporal response load in bin b across S seeds for a certain input parameter i and starting point r :

$$Y(\mathbf{U}^r) = \frac{1}{S} \sum_{s=1}^S \text{MAX}(|Y(\mathbf{U}^r)|) \quad (5)$$

3.3.2 Fatigue Loads

To compute the fatigue loads, the same basic formulation is used as for the ultimate loads, but the DEL of the temporal response is considered in place of the mean of the absolute maximums:

$$EE_{ib}^r = P(v_b) \left| \frac{DEL(\mathbf{U}^r + \mathbf{x}_k) - DEL(\mathbf{U}^r)}{\Delta_{ib}} u_{ib,range} \right| \quad (6)$$

where $DEL(\mathbf{U}^r)$ is the aggregate of the short-term DEL of a given QoI across all seeds computed using the NREL post-processing tool, MLife (Hayman et al., 2012). DELs are computed without the Goodman correction and with load ranges about a zero fixed mean. The fatigue EE value is scaled by $P(v_b)$, which is the Rayleigh probability at the wind speed v_b (assuming IEC Class IB turbulence) associated with bin b to compare the fatigue loads consistently across wind speed bins.

3.4 Identification of Most Sensitive Inputs

The EE value is a surrogate for a sensitivity level. Therefore, a higher EE value for a given input parameter indicates more sensitivity. Here, the most sensitive parameters are identified by defining a threshold over which an individual EE value would be considered significant, indicating the sensitivity of the associated parameter. This approach differs from the classical method of determining parameter sensitivity, as discussed in Appendix A. The threshold is set individually for each QoI. For the wind parameter study, the threshold is defined as $\frac{EE^r EE_{\sigma_{ib}}^r}{\sigma_{ib}} + 2\sigma$, where $\frac{EE^r EE_{\sigma_{ib}}^r}{\sigma_{ib}}$ is the mean of all EE values across all starting points R , inputs I , and wind speed bins B for each QoI Q , and σ is the standard deviation of these EE values. For the turbine parameter study, the results are stratified based on wind speed bin. Therefore, the threshold for this study is modified to $\frac{EE^r EE_{\sigma_{ib}}^r}{\sigma_{ib}} + 1.7\sigma$ due to the stratification of the results based on wind speed bin. Additionally, the ultimate load thresholds for the turbine parameter study are computed using only near- and above-rated results because of the separation of EE values between the below-, near-, and above-rated wind speed bins. However, below-rated results are included when the associated EE values occasionally exceed the threshold. For both studies, fatigue load EE values are not clearly separated by wind speed; therefore, all wind speeds are used to compute the fatigue load parameter thresholds.

4 Results

Two separate case studies were performed to assess the sensitivity of input parameters on the resulting ultimate and fatigue loads of the NREL 5-MW5-MW wind turbine. The categories of input parameters analyzed were the wind-inflow conditions and the aeroelastic turbine properties. In both of the case studies, loads were analyzed for three wind speed bins, using mean wind speed bins of 8, 12, and 18 m/s, representing below-, near-, and above-rated wind speed bins, respectively. Turbulent wind conditions were generated using an IEC Kaimal turbulence spectra with exponential spatial coherence functions. For the turbine parameter study, turbulence was based on IEC Class IB turbulence. Correlations and joint distributions of the parameters were not considered since developing this relationship for so many parameters would be difficult or impossible. In addition, the correlation could be very different for different wind sites. The impact of not considering the correlation was limited by choosing parameters that were fairly independent of one another, when possible, and by binning the results by wind speed.

4.1 Wind-Inflow Characteristics

Many researchers have examined the influence of wind characteristics on turbine load response, considering differing wind parameters and turbulence models, and using different methods to assess their sensitivity. The most common parameter considered is the influence of turbulence intensity variability, which past work has shown to have significant variability and

Formatted: Font: Not Italic

Formatted: Font: Not Italic

Formatted: Font: Not Italic

Formatted: Font: Not Italic

large impact on the turbine response (Dimitrov et al., 2015; Downey, 2006; Eggers et al., 2003; Ernst et al., 2012; Holtslag et al., 2016; Kelly et al., 2014; Matthaus et al., 2017; Moriarty et al., 2002; Rinker, 2016; Saraysoontorn et al., 2008; Sathe et al., 2012; Sutherland, 2002; Wagner et al., 2010; Walter et al., 2009). The shear exponent, or wind profile, is the next most common parameter examined, concluded to have similar or slightly less importance to the turbulence intensity (Bulaevskaya et al., 2015; Dimitrov et al., 2015; Downey, 2006; Eggers et al., 2006; Ernst et al., 2012; Kelly et al., 2014; Matthaus et al., 2017; Sathe et al., 2012). Other parameters investigated include the turbulence length scale, standard deviation of different directional wind components, Richardson number, spatial coherence, component correlation, and veer. Mixed conclusions are drawn on the importance of these secondary parameters, which are influenced by the range of variability considered (based on the conditions examined), the turbine control system, as well as the turbine size and hub height under consideration. The effects of considering the secondary wind parameters are also mixed, sometimes increasing and sometimes decreasing the loads in the turbine; however, most agree that the use of site-specific measurements of the wind parameters will lead to a more accurate assessment of the turbine loads, resulting in designs that are either better optimized or lower risk.

The focus of this case study is to obtain a thorough assessment of which wind characteristics influence wind turbine structural loads when considering the variability of these parameters over a wide sampling of site conditions.

4.1.1 Parameters

A total of 18 input parameters were chosen to represent the wind-inflow conditions, considering the mean wind profile, velocity spectrum, spatial coherence, and component correlation, as summarized in Table 2. The parameters used were identified considering a Veers model for describing and generating the wind characteristics because it provides a quantitative description with a known and limited set of inputs. Each of these parameters is described in the following sub-sections. Note that the Veers model differs from the other commonly used Mann turbulence model.¹ Regardless, the Veers model is used here because it is more tailorable than the Mann model, *i.e.*, there are more input parameters that can be varied.

Table 2. Wind-inflow condition parameters (18 total).

| Mean Wind Profile | Velocity Spectrum | Spatial Coherence | Component Correlation |
|--------------------|---|--|---|
| Shear (σ) | Standard deviation, u ($\sigma_u, \sigma_v, \sigma_w$) | Input coherence decrement, u (a_u, a_v, a_w) | Reynolds stress, uw ($PC_{uw}, PC_{uv}, PC_{vw}$) |
| Veer (β) | Integral scale parameter, u (L_u, L_v, L_w) Standard deviation, v (σ_v) | Input coherence decrement, v Offset parameter, (b_u, b_v, b_w) (a_v) | Reynolds stress, uv (PC_{uv}) |
| | Standard deviation, w (σ_w) | Exponent (γ) Input coherence decrement, w (a_w) | Reynolds stress, vw (PC_{vw}) |
| | Integral scale parameter, u (L_u) | Offset parameter, u (b_u) | |
| | Integral scale parameter, v (L_v) | Offset parameter, v (b_v) | |
| | Integral scale parameter, w (L_w) | Offset parameter, w (b_w) | |
| | | Exponent (γ) | |

Formatted: Font color: Auto, Not Superscript/ Subscript

Formatted: Font color: Auto, Not Superscript/ Subscript

Formatted: Font color: Auto

Formatted: Font color: Auto, Not Superscript/ Subscript

¹ The Mann turbulence model (also considered in the IEC 61400-1 standard) is based on a three-dimensional tensor representation of the turbulence derived from rapid distortion of isotropic turbulence using a uniform mean velocity shear (Jonkman, 2009). The Mann model considers the three turbulence components as dependent, representing the correlation between the longitudinal and vertical components resulting from the Reynolds stresses. In the IEC 61400-1 standard, the two spectra (Mann and Kaimal) are equated, resulting in three parameters that may be set for the Mann model. However, there is uncertainty in whether the loads resulting from these two different turbulence spectra are truly consistent.

4.1.1.1 Mean Wind Profile

A standard power-law shear model is used to describe the vertical wind speed profile and a linear wind direction veer model is used. The sensitivity of these characteristics are captured through variation of the exponent of the shear, α , and the total veer across the turbine, β (centered around the hub, following right-hand-rule about the vertical axis of the turbine). The IEC 61400-1 standard (IEC, 2005) uses $\alpha = 0.2$ and $\beta = 0^\circ$ under normal turbulence.

4.1.1.2 Velocity Spectrum

The Veers model uses a Kaimal spectrum to represent the turbulence. The Kaimal spectrum is defined as (IEC, 2005):

$$\frac{fS_q(f)}{\sigma_q^2} = \frac{4fL_q/V_{\text{hub}}}{(1 + 6fL_1/V_{\text{hub}})^{5/3}} \quad (7)$$

where f is the frequency, q is the index of the velocity component direction (u, v, w), S_q is the single-sided velocity spectrum, V_{hub} is the mean wind speed at hub height, σ_q is the velocity component standard deviation, and L_q is the velocity component integral scale parameter. The IEC 61400-1 standard (IEC, 2005) uses a wind-speed-dependent standard deviation, i.e., $\sigma_u = 0.14 \times (0.75V_{\text{hub}} + 5.6 \text{ m/s})$, and a set scaling between the direction components of the standard deviation and scale parameters, i.e., $\sigma_v = 0.8\sigma_u$; $\sigma_w = 0.8\sigma_u$; $L_u = 8.1 \times (42 \text{ m}) = 340.2 \text{ m}$; $L_v = 2.7 \times (42 \text{ m}) = 113.4 \text{ m}$; and $L_w = 0.66 \times (42 \text{ m}) = 27.72 \text{ m}$. However, in this study each parameter in (u, v, w) is varied independently. An inverse Fourier transform is applied to the Kaimal spectrum and random phases derived from the turbulence seed to derive a turbulent time series for each of the wind components independently.

4.1.1.3 Spatial Coherence Model

The point-to-point spatial coherence (Coh) quantifies the frequency-dependent cross-correlation of a single turbulence component at different transverse points in the wind inflow grid. The general coherence model used in TurbSim is defined as:

$$Coh_{q,i,j} = \exp\left(-a_q \left(\frac{d}{z_m}\right)^\gamma \sqrt{\left(\frac{fd}{V_{\text{hub}}}\right)^2 + (b_q d)^2}\right) \quad (8)$$

where d is the distance between points i and j , z_m is the mean height of the two points (IEC, 2005), and V_{hub} is the mean wind speed at hub height. The variables a_q and b_q are the input coherence decrement and offset parameter, respectively. Note that the use of V_{hub} in the general coherence model is a modification to the standard TurbSim method. The model is based on the IEC coherence model with the added term-factor $(d/z_m)^\gamma$ – introduced by Solari (1987) – where γ can vary between 0 and 1. The IEC 61400-1 standard (IEC, 2005) does not use the $(d/z_m)^\gamma$ term-factor and uses $a_u = 12$ and $b_u = 0.12/L_u$. Coherence is not defined in the standard (IEC, 2005) for the transverse wind components v and w.

4.1.1.4 Component Correlation Model

The component-to-component correlation (PC) quantifies the cross-correlation between directional turbulence components at a single point in space. For example, PC_{uw} quantifies the correlation between the u and w turbulence components at a given point. TurbSim modifies the v- and w-component wind speeds by computing a linear combination of the time series of the three independent wind speed components to obtain the mean Reynolds stresses (PC_{uw} , PC_{uv} , and PC_{vw}) at the hub. Note that because this calculation occurs in the time domain, the velocity spectra of the v- and w-components are somewhat affected by the enforced component correlations. The IEC 61400-1 standard (IEC, 2005) does not specify Reynolds stresses.

Formatted: Font: Not Italic

Formatted: Font color: Auto

Formatted: Font color: Auto

Formatted: Font color: Auto

4.1.2 Parameter Ranges

To assess the sensitivity of each of the parameters on the load response, a range over which the parameters could vary was defined. The variation level was assessed through a literature search seeking the range over which the parameters could realistically vary for different wind-farm sites around the world (Berg et al., 2013; Bulaevskaya et al., 2015; Clifton; Dimitrov et al., 2016; Dimitrov et al., 2015; Eggers et al., 2003; Ernst et al., 2012; Holtslag et al., 2016; Jonkman, 2009; Kalverla et al., 2017; Kelley, 2011; Lindelöw-Marsden, 2009; Matthaus et al., 2017; Moriarty et al., 2002; Moroz, 2017; Nelson et al., 2003; Park et al., 2015; Rinker, 2016; Saint-Geours et al., 2010; Saranyasontoom et al., 2004; Saranyasontoom et al., 2008; Sathe et al., 2012; Solari, 1987; Sutherland, 2002; Teunissen, 1970; Wagner et al., 2010; Walter et al., 2009; Wharton et al., 2015; Ziegler et al., 2016). When possible, parameter ranges were set based on wind speed bins. If no information on wind-speed dependence was found, the same values were used in all bins. The ranges, summarized in Table 3, were taken from multiple sources (references cited below the values), based on measurements across a variety of different locations and conditions. For comparison, the nominal value prescribed by IEC for category B turbulence is specific in the “Nom” row.

To simplify the screening of the most influential parameters, all parameters were considered independent of one another. This was done because of the difficulty of considering correlations between a large number of parameters. Such correlations should be studied in future work once parameter importance has been established. Since each parameter was considered independently, except for the conditioning on wind speed bin, some non-physical parameter combinations may arise. This was considered acceptable for the screening process.

4.1.3 Elementary Effects

The EE value was calculated for each of the 18 input parameters (I) at 30 different starting points (R) in the input-parameter hyperspace. The number of points was determined through a convergence study on the average of the EE value. At each of the points examined, S different turbulent wind files (i.e. S independent time-domain realizations from S seeds) were run. Thirty seeds were needed based on a convergence study of the ultimate and fatigue load metrics for all QoIs. Based on these numbers, the total number of simulations performed for the wind-inflow case study was $R \times (I+1) \times S \times B = 30 \times 19 \times 30 \times 3 = 51,300$, where B is the number of wind speed bins considered.

The EE values across all input parameters, input hyperspace points, and wind speed bins were examined for each of the QoIs for ultimate and fatigue loads. To identify the most sensitive parameters, a tally was made of the number of times an EE value exceeded the threshold for a given QoI. The resulting tallies are shown in Figure 3, with the ultimate load tally on the left and the fatigue load tally on the right. As expected, these plots show an overwhelming level of sensitivity of the u-direction turbulence standard deviation (σ_u) and also the vertical wind shear (α). However, focusing on the lower tally values in this plot (shown in) highlights the secondary-level of importance of veer (β), u-direction integral length (L_u) and components of the IEC coherence model (a_u and b_u), as well as the exponent (γ).

Table 3: Included wind-inflow parameter ranges separated by wind speed bin.

| | α (-) | β (deg) | L_u (m) | L_v (m) | L_w (m) | σ_u (m/s) | σ_v (m/s) | σ_w (m/s) | a_u (-) | a_v (-) | a_w (-) | b_u (m ³) | b_v (m ³) | b_w (m ³) | γ (-) | PC_{uw} (m ² /s ²) | PC_{uv} (m ² /s ²) | PC_{vw} (m ² /s ²) |
|---|-----------------|------------------|--------------|--------------|--------------|---------------------|---------------------|---------------------|--------------|--------------|--------------|----------------------------|----------------------------|----------------------------|-----------------|--|--|--|
| Below-rated wind speed, 3-10 m/s | | | | | | | | | | | | | | | | | | |
| Nom. | 0.2 | 0 | 340 | 110 | 28 | 1.6 | 1.3 | 1.3 | 12 | - | - | 3.5E-4 | - | - | 0 | - | - | - |
| Min. | -1.5* | -25 | 5 | 2 | 2 | 0.05 | 0.02 | 0.03 | 1.5 | 1.7 | 2 | 0 | 0 | 0 | 0 | -3.5 | -4.5 | -2.7 |
| Max. | 3.3 | 50 | 1,000 | 1,000 | 650 | 7.2 | 7.4 | 4.5 | 26 | 18 | 17 | 0.08 | 4.5E-3 | 0.011 | 1 | 0.50 | 6.0 | 1.0 |

| Ref. | Clifton | Walter et al., 2009 | Nelson et al., 2003; Solari et al., 2001 | Nelson et al., 2003 | Nelson et al., 2003; Teunissen, 1970 | Clifton | Clifton | Clifton | Solari 1987 | Saranyaasoontorn et al., 2006 | Solari 1987; Solari et al., 2001 | Saranyaasoontorn et al., 2004 | Jonkman 2009 | Jonkman 2009 | Solari 1987 | Kelley 2011 | Kelley 2011 | Kelley 2011 |
|--|-----------------------------------|--|--|---------------------|--------------------------------------|---|---|---|-------------|-------------------------------|--|-------------------------------|--------------|--------------|-------------|-------------|-------------|-------------|
| Near-rated wind speed, 10-14 m/s | | | | | | | | | | | | | | | | | | |
| Nom. | 0.2 | 0 | 340 | 110 | 28 | 2.0 | 1.6 | 1.6 | 12 | - | - | 3.5E-4 | - | - | 0 | - | - | - |
| Min. | -0.4 | -10 | 8 | 2 | 2 | 0.20 | 0.05 | 0.05 | 1.5 | 1.7 | 2 | 0 | 0 | 0 | -3.5 | -4.5 | -2.7 | - |
| Max. | 0.9 | 50 | 1,400 | 1,300 | 450 | 7.3 | 8.1 | 4.3 | 26 | 18 | 17 | 0.08 | 3.0E-3 | 6.0E-3 | 1 | 0.50 | 6.0 | 1.0 |
| Ref. | Dimitrov et al., 2015; Moroz 2017 | Dimitrov et al., 2015; Walter et al., 2009 | Nelson et al., 2003; Solari et al., 2001 | Nelson et al., 2003 | Nelson et al., 2003 | Clifton; Kelley 2011 | Clifton; Kelley 2011 | Clifton; Kelley 2011; Nelson et al., 2003 | Solari 1987 | Saranyaasoontorn et al., 2006 | Saranyaasoontorn et al., 2006; Solari 1987 | Saranyaasoontorn et al., 2004 | Jonkman 2009 | Jonkman 2009 | Solari 1987 | Kelley 2011 | Kelley 2011 | Kelley 2011 |
| Above-rated wind speed, 14-25 m/s | | | | | | | | | | | | | | | | | | |
| Nom. | 0.2 | 0 | 340 | 110 | 28 | 2.7 | 2.1 | 2.1 | 12 | - | - | 3.5E-4 | - | - | 0 | - | - | - |
| Min. | -0.4 | -10 | 25 | 2 | 2 | 0.20 | 0.18 | 0.15 | 1.5 | 1.7 | 2 | 0 | 0 | 0 | -3.5 | -4.5 | -2.7 | - |
| Max. | 0.7 | 25 | 1,600 | 1,500 | 650 | 7.4 | 7.3 | 4.2 | 26 | 18 | 18 | 0.05 | 2.5E-3 | 6.5E-3 | 1 | 0.50 | 6.0 | 1.0 |
| Ref. | Dimitrov et al., 2015; Moroz 2017 | Dimitrov et al., 2015; Walter et al., 2009 | Kelly et al., 2014; Nelson et al., 2003 | Nelson et al., 2003 | Nelson et al., 2003 | Clifton; Kelley 2011; Nelson et al., 2003 | Clifton; Kelley 2011; Nelson et al., 2003 | Clifton; Kelley 2011; Nelson et al., 2003 | Solari 1987 | Saranyaasoontorn et al., 2006 | Jonkman 2009; Solari et al., 2001 | Saranyaasoontorn et al., 2004 | Jonkman 2009 | Jonkman 2009 | Solari 1987 | Kelley 2011 | Kelley 2011 | Kelley 2011 |

* This value was changed to -0.75 due to simulation issues

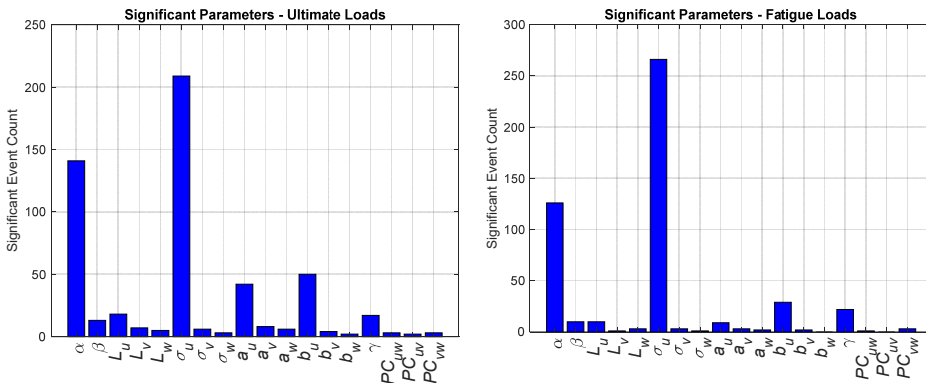


Figure 3: Identification of significant parameters using ultimate (left) and fatigue (right) loads. Significant events are defined by number of outliers identified across each of the QoIs for all wind speed bins, input parameters, and simulation points.

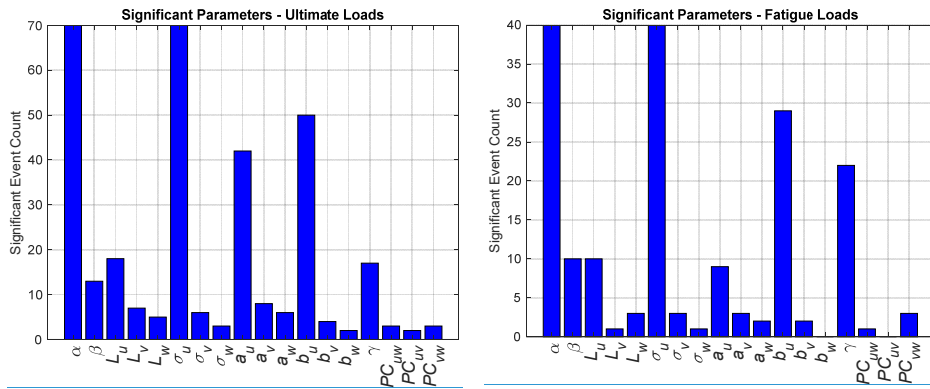


Figure 4: Zoomed-in view of identification of significant parameters using ultimate (left) and fatigue (right) loads.

Exceedance probability and Histograms of the EE values for each of the QoIs are plotted in Figure 4, and Figure 5 for the ultimate and fatigue load metrics (associated exceedance probability plots are shown in Appendix B, Figure 21 and Figure 22). Each plot contains all calculated EE values for a given QoI colored by wind speed bin. The threshold used to identify significant EE values is shown in each plot as a solid black line. All points above the threshold line indicate a significant event and are included in the outlier tally for each QoI. Note that while electric power is shown, it is not used in the outlier tally because its variation is strictly limited by the turbine controller rather than other wind parameters. Highlighted in these figures is that most of the outliers come from the below-rated wind speed bin.

- 5
- 10 To understand why the below-rated wind speed bin would be creating the most outliers, a more thorough examination is made for one of the QoIs. Exceedance probability plots of blade-root loads are shown in Figure 6. Here, all input parameters are plotted independently of each other to compare the behavior between parameters. Each line represents a different input parameter, with each point representing a different location in the hyperspace. These plots show how the shear and u-component standard deviation for the lower wind speed bin stand-out compared to all other parameters; likewise, the u-component standard deviation stands out across different wind speed bins for the ultimate load. One of the reasons that the shear value shows such a large sensitivity in the lowest wind speed bin is the large range over which the parameter is varied. A smaller range is used for the near- and above-rated bins, resulting in less sensitivity to shear for those wind speeds. The impact of the range on the sensitivity of the parameter indicates that for sites with extreme conditions, such as an extreme shear, using appropriate parameter values in a loads analysis can be important in accurately assessing the ultimate and fatigue loading on the turbine. The effect of shear could also be diminished by employing independent blade-pitch control, whereas the reference NREL 5-MW-5-MW turbine controller used here employs collective blade-pitch control.

25 Histogram plots of blade-root bending moment EE values are shown in Figure 7 and Figure 8. In each figure, wind speed bins are displayed in different plots and EE value histograms showing the contribution from all input parameters are shown in each histogram. Ultimate load EE values are shown in Figure 7 and fatigue load EE values are shown in Figure 8. Highlighted in these plots is the large sensitivity of the shear parameter and, to a lesser extent, u-component standard deviation in the far extremes.

- Field Code Changed
- Field Code Changed
- Field Code Changed
- Field Code Changed
- Field Code Changed

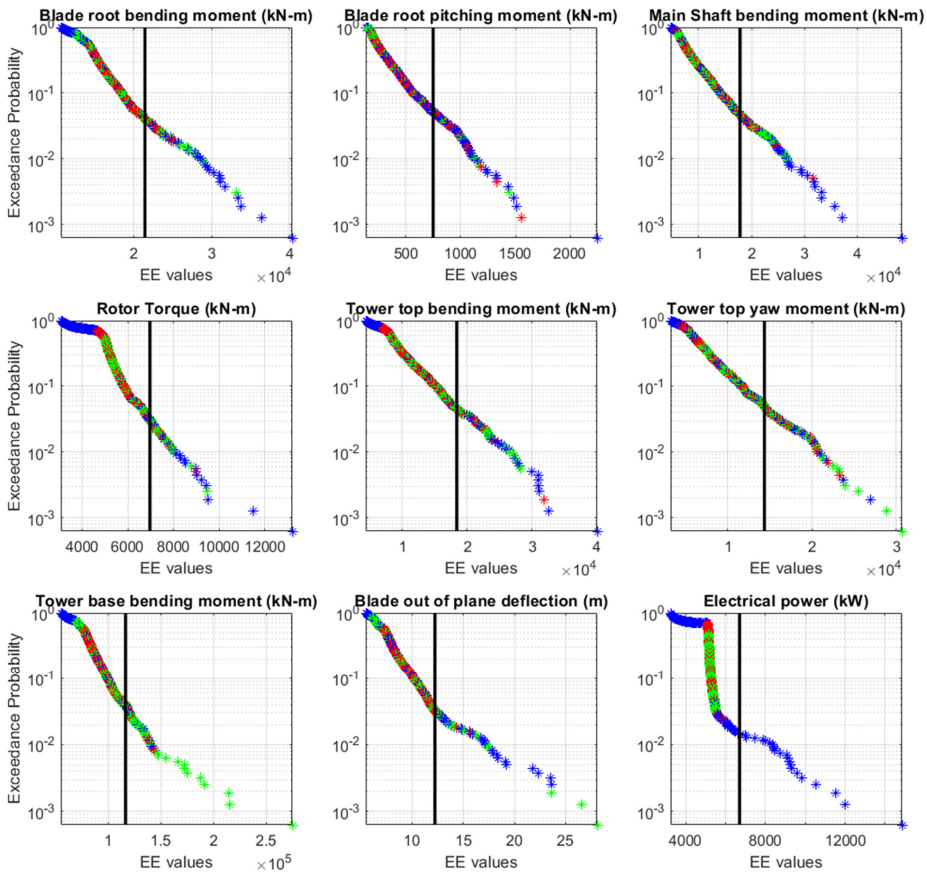


Figure 5: Exceedance probability plot of ultimate load EE values for each of the QoIs across all wind speed bins, input parameters, and simulation points. Black line represents the defined threshold by which outliers are counted for each QoI. Color indicates wind speed bin (blue=below rated, red=near rated, green=above rated).

Formatted: Justified, Don't keep with next

Formatted: Normal

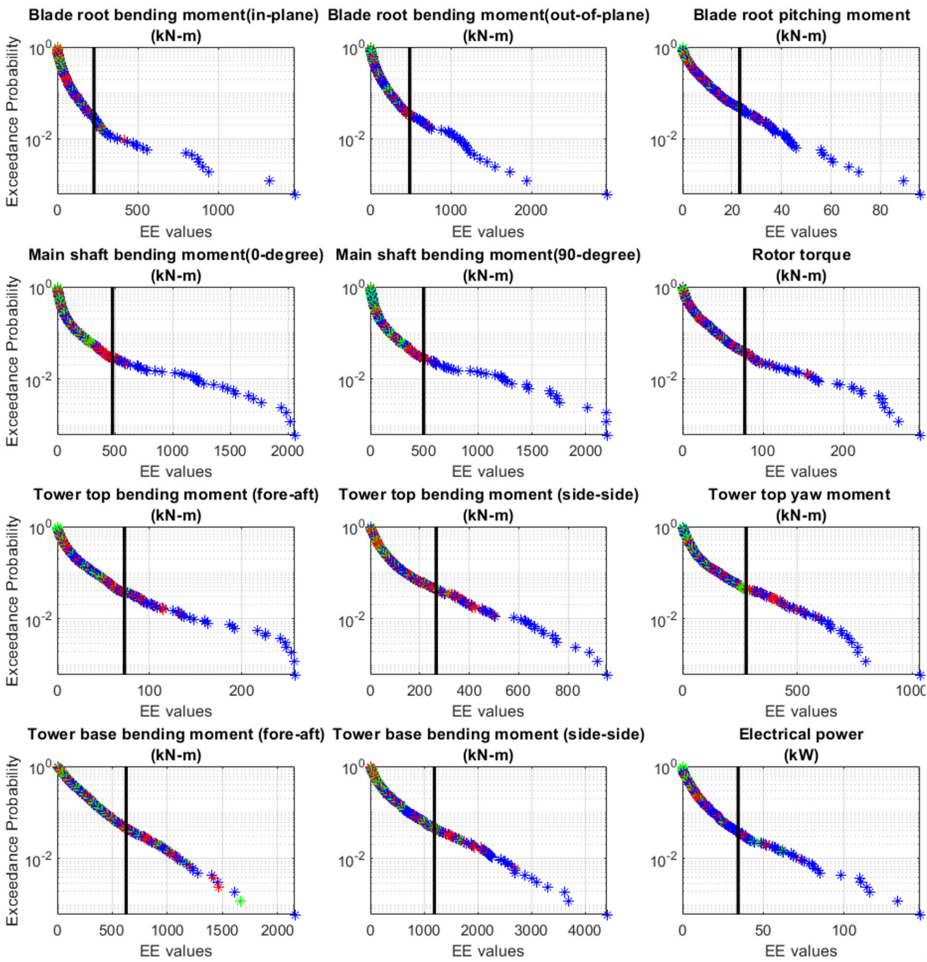


Figure 6: Exceedance probability plot of fatigue load EE values for each of the across all wind speed bins, input parameters, and simulation points. Black line represents the defined threshold by which outliers are counted for each QoI. Color indicates wind speed bin (blue=below-rated, red=near-rated, green=above-rated).

Formatted: Justified, Don't keep with next

Formatted: Normal

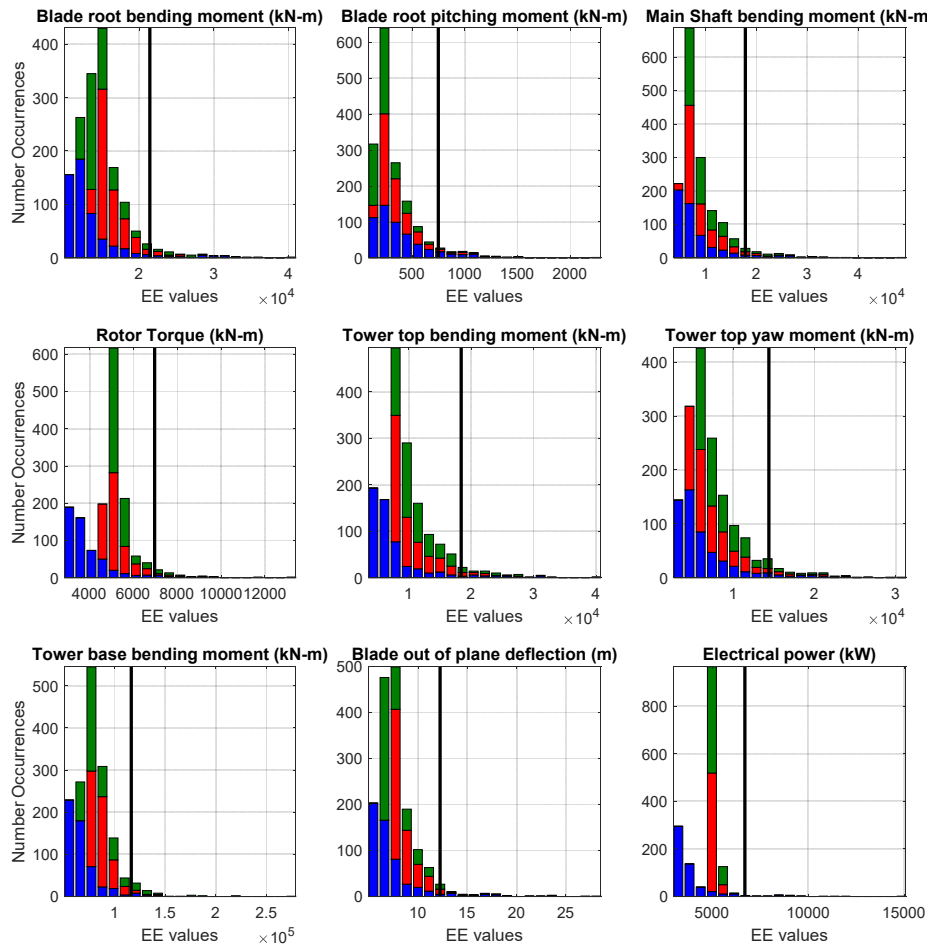


Figure 4: Stacked histogram of the ultimate load EE values for each of the QoIs across all wind speed bins, input parameters, and simulation points. Black line represents the defined threshold by which outliers are counted for each QoI. Color indicates wind speed bin (blue=below rated, red=near rated, green=above rated).

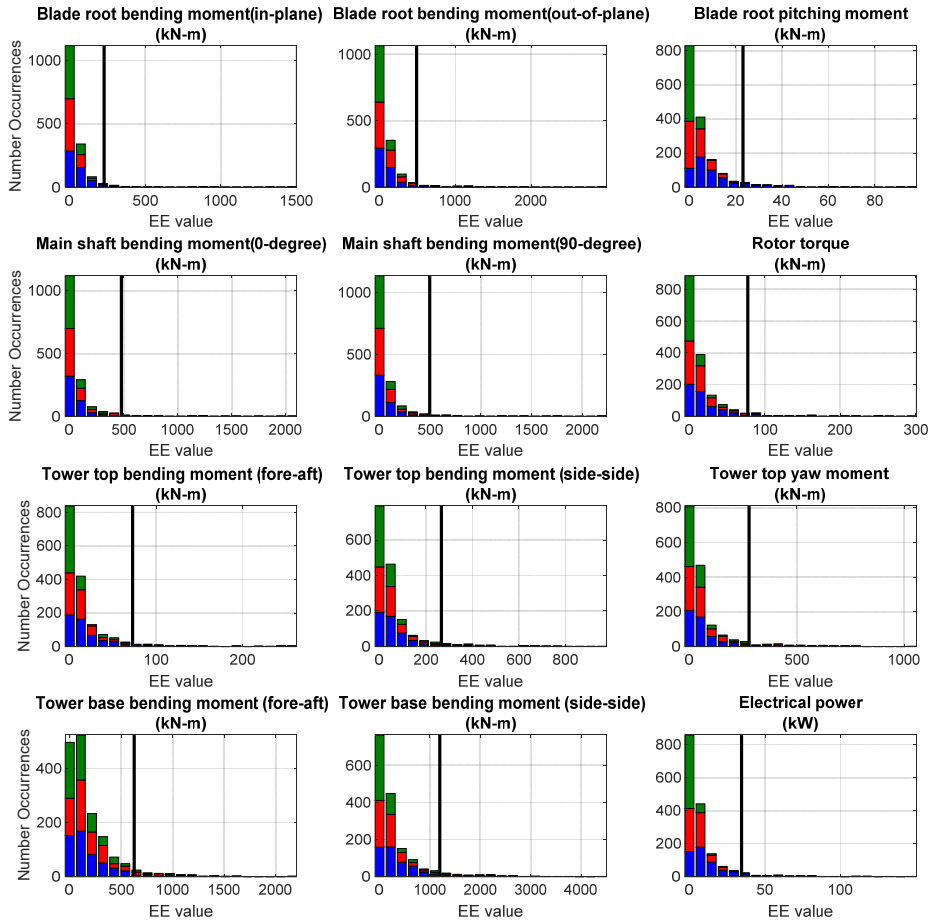


Figure 5: Stacked histogram of the fatigue load EE values for each of the QoLs across all wind speed bins, input parameters, and simulation points. Black line represents the defined threshold by which outliers are counted for each QoL. Color indicates wind speed bin (blue=below rated, red=near rated, green=above rated).

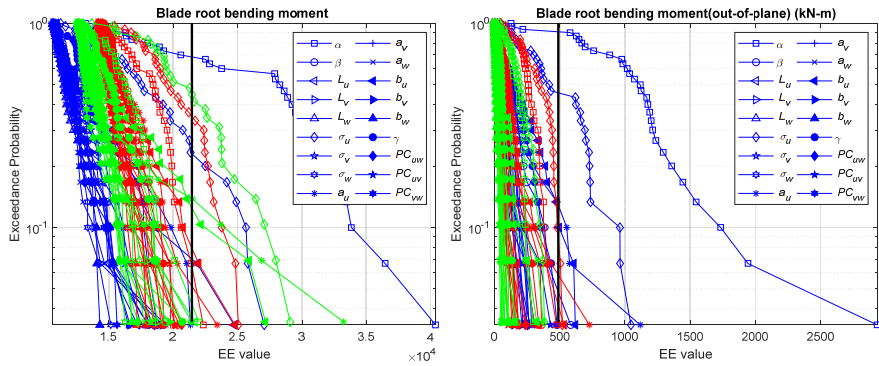


Figure 6: Exceedance probability plot of ultimate (left) and fatigue (right) load EE values for blade-root bending moments. Each line represents a different input parameter and wind speed bin (blue=below rated, red=near rated, green=above rated).

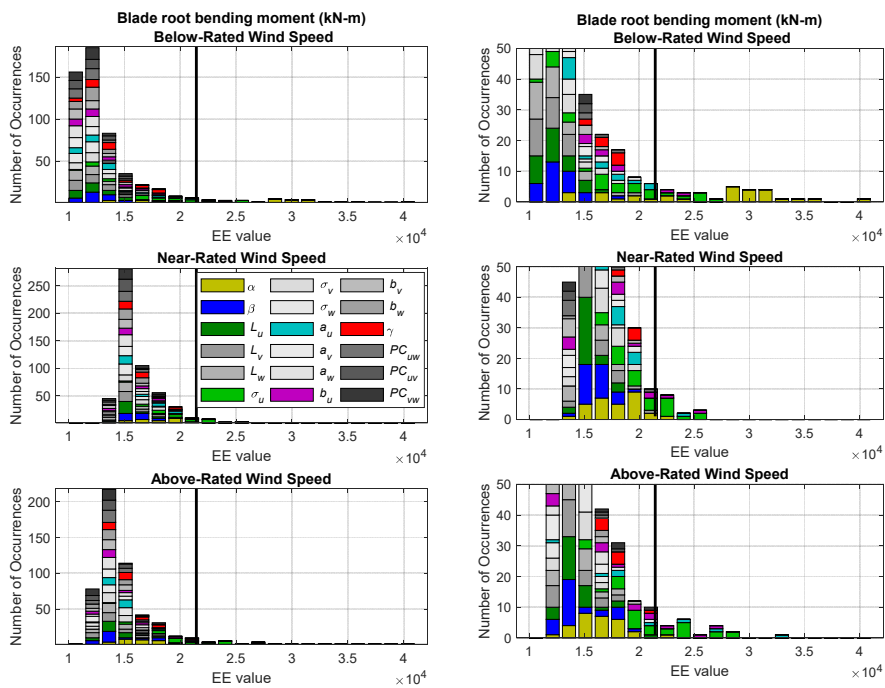


Figure 7: Histogram of ultimate load EE values for the blade-root bending moment. Each graph (in left column) shows one wind speed bin and includes all input parameters. Right column is a zoom of the left.

5

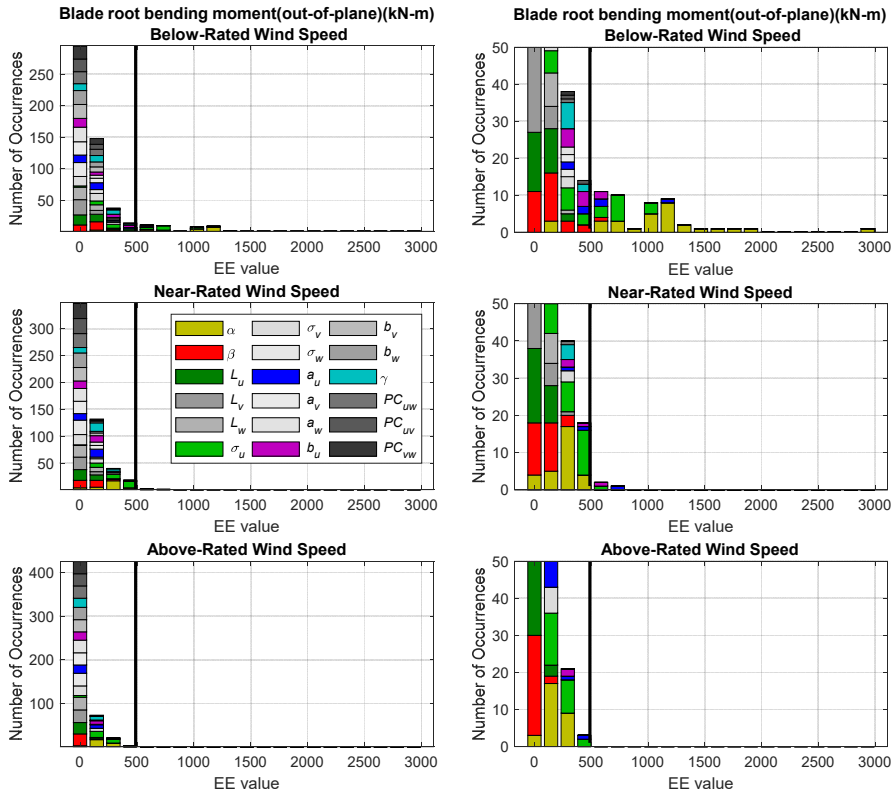


Figure 8: Histogram of fatigue load EE values for the blade-root bending out-of-plane bending moment. Each graph (in left column) shows one wind speed bin and includes all input parameters. Right column is a zoom of the left.

To summarize which parameters are important for which QoIs, the number of times each input parameter contributed to the significant event count for a given QoI was tallied. The top most sensitive parameters are shown in Table 4 and Table 5 for ultimate and fatigue loads, respectively. Overall, 46% of the outliers for both ultimate and fatigue loads are due to u-direction turbulence standard deviation (σ_u), and 26% for vertical shear (α), and for all but two outputs QoIs, these are the most sensitive parameters. The two exceptions are blade-root pitching moment and tower-base bending moment, which show u-direction turbulence standard deviation as the most important parameter, but show coherence properties and integral scale parameter as more important than shear. This is understandable since shear will have little effect on collective blade pitching and rotor thrust. The remaining parameters have far less significance, with only components of the IEC coherence model, a_u (5%) and b_u (8%), having a value great than 1%. These results can be used in future sensitivity analysis work to focus on perturbation of specific input parameters based on desired turbine loads.

Table 4. Top input parameters contributing to ultimate load sensitivity of each QoI. Values indicate how many times the variable contributes to the sensitivity count.

| Blade-Root Bending Mom. | Blade-Root Pitch Mom. | Main Shaft Bending Mom. | Rotor Torque | Tower-Top Bending Mom. | Tower-Top Yaw Mom. | Tower-Base Bending Mom. | Blade OoP Deflection |
|-------------------------|-----------------------|-------------------------|-----------------|------------------------|--------------------|-------------------------|----------------------|
| σ_u (29) | σ_u (26) | α (33) | σ_u (28) | α (31) | σ_u (41) | σ_u (22) | α (22) |
| α (22) | γ (10) | σ_u (28) | α (12) | σ_u (22) | α (10) | a_u, b_u, L_u (8) | σ_u (13) |
| b_u (7) | L_u (8) | a_u, b_u (5) | b_u (6) | a_u, b_u (5) | a_u, b_u (8) | -- | b_u (9) |

Table 5. Top input parameters contributing to fatigue load sensitivity of each QoI. Values indicate how many times the variable contributes to the sensitivity count.

| Blade-Root IP Bend. Moment | Blade-Root OP Pitch. Moment | Blade-Root Pitch. Moment | Main Shaft Bending Moment 0° | Main Shaft Bending Mom. 90° | Rotor Torque | Tower-Top FA Bend. Moment | Tower-Top SS Bend. Moment | Tower-Top Yaw Moment | Tower-Base FA Bend. Moment | Tower-Base SS Bend. Moment |
|----------------------------|-----------------------------|--------------------------|------------------------------|-----------------------------|-----------------|---------------------------|---------------------------|----------------------|----------------------------|----------------------------|
| σ_u (10) | α (14) | σ_u (14) | α (18) | α (18) | σ_u (25) | σ_u (31) | σ_u (47) | σ_u (48) | σ_u (24) | σ_u (35) |
| α (8) | σ_u (9) | L_u (7) | σ_u (12) | σ_u (11) | α (11) | α (12) | α (13) | α (12) | α (6) | α (9) |
| b_u (3) | b_u (4) | α (5) | β (2) | β (2) | b_u (9) | b_u (7) | γ (3) | γ (3) | γ (4) | γ (4) |

4.2 Aeroelastic Turbine Properties

The second case study focuses on which aeroelastic turbine parameters have the greatest influence on turbine ultimate and fatigue loads during normal turbine operation. These properties are categorized into four main categories: support structure, blade structural, blade aerodynamic, and controller properties.

It is widely acknowledged that uncertainty in the aerodynamic parameters can affect the prediction of turbine performance and structural loading (Abdallah et al., 2015; Madsen et al., 2010; Simms et al, 2001). Abdallah et al. (2015) demonstrated the impact of uncertainty in steady airfoil data on prediction of extreme loads and assessed the correlation between various static coefficient polars (Abdallah et al., 2015). Despite significant work to measure these parameters, considerable uncertainty remains in their prediction. Static lift and drag measurements almost exclusively come from wind tunnel tests of airfoils, which lack three-dimensional and unsteady effects that are instead estimated through the application of semi-empirical engineering models, e.g., rotational augmentation (stall delay) and stall hysteresis (Abdallah et al., 2015, Simms et al, 2001). In Damiani (2010), unsteady aerodynamic parameters were tuned for several airfoil sections to match experimental lift and drag unsteady hysteresis loops, but the consequences of parameter variation were not considered. Blade chord and twist ranges were chosen using the work of Loeven and Bihl (2008), who identified changes in blade chord and twist based on uncertainty in aerodynamic loading, icing, or wear of the blades.

Beyond the blade aerodynamic properties, other turbine properties also contribute to the uncertainty of the load response characteristics. Abdallah (2015) provides a comprehensive assessment of the sources of uncertainty affecting the prediction of loads in a wind turbine. Researchers have not focused on these other parameters as significantly as the aerodynamic ones, but they could have a significant contribution to the uncertainty. Witcher (2017) examined uncertainty in properties such as the tower and blade mass/stiffness properties within the context of defining a probabilistic approach to designing wind turbines by examining distributions of the load from propagated input parameter uncertainties versus resistance distributions. Prediction of the reliability of the wind turbine has been studied through examination of the damping in the structure by Koukoura (2014) and a better understanding of the uncertainty in the properties of the drivetrain by Holierhoek (2010). Limited information is available on what the actual ranges of uncertainty are for these different characteristics. For most studies, expert opinion is used to set a realistic bound. A better assessment of these bounds will be needed in future work to understand the relative importance of the physical parameters and to provide a more precise assessment of the uncertainty bounds in the load response of wind turbines.

4.2.1 Parameters

For the turbine aeroelastic properties, 39 input parameters were identified covering support structure properties, blade structural properties, blade aerodynamic properties (both steady and unsteady characteristics), and controller properties. These parameters are summarized in Table 6. (acronyms are defined in the following subsections).

Table 6. Turbine aeroelastic parameters (39 total).

| Support Structure Properties | Blade Structural Properties | Blade Aerodynamic Properties | Controller Properties |
|------------------------------------|--|---|---|
| Nacelle mass (N_{Mass}) | Blade flapwise stiffness (B_{FWS}) | Twist (θ) at tip | Yaw Angle Error (θ) |
| Nacelle CM x-location (N_{CM}) | Blade edgewise stiffness (B_{EWS}) | Chord (c) at root and tip | Collective pitch error ($\theta_{err, coll}$) |
| Tower CM location (T_{CM}) | Blade flapwise stiffness imbalance ($B_{FK, imb}$) | Leading-edge separation time constant (T_{θ}) | Imbalanced pitch error ($\theta_{err, imb}$) |
| Tower stiffness (T_{KFS}) | Blade edgewise stiffness imbalance ($B_{EK, imb}$) | Vortex shedding time constant (T_{VS}) | |
| Tower mass (T_{MS}) | Blade damping ratio (B_{DR}) | Leading-edge pressure gradient time constant (T_{ρ}) | |
| Tower damping ratio (T_{DR}) | Blade mass (B_{M}) | Vortex advection time constant (T_{VA}) | |
| Drivetrain stiffness (D_K) | Blade mass imbalance ($B_{M, imb}$) | Strouhal Number (St_{ρ}) | |
| Drivetrain damping (D_R) | Blade CM location (B_{CM}) | Lift (C_L) at root and tip | |
| Shaft angle (α_S) | Precone (β_P) | TES Lift AoA (α_{TES}) | |
| | | -- at root and tip -- | |
| | | Max Lift AoA (α_{max}) | |
| | | -- at root and tip -- | |
| | | SR Lift AoA (α_{SR}) | |
| | | -- at root and tip -- | |
| | | 0-degree drag ($C_{d,0}$) | |
| | | -- at root and tip -- | |

4.2.2 Parameter Ranges

The level of variation was based on the perceived level of uncertainty in the parameter values. Some of these levels of uncertainty are proposed within the literature, but when no other information was available, expert opinion was used. The source for the information is provided below the values in each table summarizing the parameter ranges. "Exp" is used to identify where expert opinion was used. The uncertainty levels are largely percentage based, but in some instances an exact value was used. The following sub-sections define the ranges of the parameters introduced in . All parameters were considered independent of one another, as was done for the wind parameter sensitivity analysis.

Table 6. Turbine aeroelastic parameters (39 total).

| Support Structure Properties | Blade Structural Properties | Blade Aerodynamic Properties | Controller Properties |
|------------------------------|--|-------------------------------|------------------------------|
| Nacelle mass (N_{Mass}) | Blade flapwise stiffness (B_{FWS}) | Twist (θ) at tip | Yaw Angle Error (θ) |
| Nacelle CM | Blade edgewise | Chord (c) at root and tip | Collective pitch |

Field Code Changed

Formatted: Font: (Default) Times New Roman

Formatted: ... [1]

Formatted: ... [2]

Formatted: Font: (Default) Times New Roman

Formatted: Font: (Default) Times New Roman

Formatted: ... [3]

Formatted: ... [4]

Formatted: ... [5]

Formatted: Font: (Default) Times New Roman

Formatted: ... [6]

Formatted: ... [7]

Formatted: ... [8]

Formatted: ... [9]

Formatted: ... [10]

Formatted: ... [11]

Formatted: ... [12]

Formatted: ... [13]

Formatted: Font: (Default) Times New Roman

Formatted: ... [15]

Formatted: ... [14]

Formatted: ... [16]

Formatted: ... [17]

Formatted: ... [19]

Formatted: ... [18]

Formatted: ... [20]

Formatted: ... [21]

Formatted: ... [22]

Formatted: ... [23]

Formatted: Font: (Default) Times New Roman

Formatted: Font: (Default) Times New Roman

Formatted: ... [24]

Formatted: Font: (Default) Times New Roman

Formatted: ... [25]

Formatted: Font: (Default) Times New Roman

Formatted: ... [26]

Formatted: Font: (Default) Times New Roman

| | | | |
|-----------------------------------|---|---|---|
| x -location (N_{CM}) | stiffness (B_{st}) | | error ($\theta_{off,roll}$) |
| Tower CM location (T_{CM}) | Blade flapwise stiffness imbalance ($B_{FK,imb}$) | Leading edge separation time constant (T_{LE}) | Imbalanced pitch error ($\theta_{off,imb}$) |
| Tower stiffness (T_{st}) | Blade edgewise stiffness imbalance ($B_{EK,imb}$) | Vortex shedding time constant (T_{VSD}) | |
| Tower mass (T_{MD}) | Blade damping ratio (B_{DR}) | Leading edge pressure gradient time constant (T_{LE}) | |
| Tower damping ratio (T_{DR}) | Blade mass (B_{M}) | Vortex advection time constant (T_{VA}) | |
| Drivetrain stiffness (D_{st}) | Blade mass imbalance ($B_{M,imb}$) | Strouhal Number (St_{SH}) | |
| Drivetrain damping (D_{DR}) | Blade CM location (B_{CM}) | Lift (C_L) at root and tip | |
| Shaft angle (α_s) | Precone (β_{pr}) | TES Lift AoA (α_{TES}) at root and tip | |
| | | Max Lift AoA (α_{max}) at root and tip | |
| | | SR Lift AoA (α_{SR}) at root and tip | |
| | | 0 degree drag ($C_{d,0}$) at root and tip | |

Formatted: Justified

4.2.2.1 Support Structure Properties

For the support structure, 9 parameters were varied and summarized in **Error! Not a valid bookmark self-reference.** These parameters included mass and center of mass (CM) of the tower and nacelle; tower and drivetrain stiffness factors; tower and drivetrain damping ratio; and shaft angle. To manipulate the tower structural response, the frequency of the corresponding tower mode shapes was changed by $\pm 15\%$ of 0.32 Hz by uniformly scaling the associated stiffness. While tower stiffness is specified as a factor by which mode shapes are scaled, the drivetrain stiffness is entered directly. Note that the mode shapes themselves (which are specified independently of the mass and stiffness in ElastoDyn) were not changed in this process. The tower mass was changed by varying the distributed tower mass density factory. The tower CM location was changed by varying the tower-base and -top density such that density increased at one end and decreased at the other without changing the overall blade mass. The drivetrain damping term represents the combined effect of structural damping and drivetrain damping from active control.

Table 7: Parameter value ranges of turbine support structure parameter ranges.

| | N_{mass} (kg) | N_{CM} (m) | T_{CM} (m) | T_{KF} (-) | T_{MD} (-) | T_{DR} (%) | D_K $\left(\frac{N \cdot m}{rad}\right)$ | D_D $\left(\frac{N \cdot m}{rad/sec}\right)$ | α_s (deg) |
|-------------|--------------------|-----------------|-----------------|-----------------|-----------------|-----------------|---|---|--------------------------|
| Nom. | 240,000 | 1.9 | 42.505 | 1.02 | 1 | 2.55 | 867,637,000 | 6,215,000 | -5 |
| Min. | 216,000 | 1.71 | 40.38 | 0.72 | 0.95 | 0.1 | 780,873,300 | 0.0 | -5.2 |
| Max. | 264,000 | 2.09 | 44.63 | 1.32 | 1.05 | 5.0 | 954,400,700 | 12,430,000 | -4.8 |
| Ref. | Witcher, 2017 | Exp | Exp | Koukoura 2014 | Witcher, 2017 | Koukoura 2014 | Holierhoek et al., 2010 | Holierhoek et al., 2010 | Santos and van Dam, 2015 |

4.2.2.2 Blade Structural Properties

For the blade structural properties, 9 parameters were considered, including blade flapwise and edgewise stiffness (including stiffness imbalance), mass (including mass imbalance), CM, damping, and precone angle, as detailed in Table 8. Through ElastoDyn, blade structural dynamics are modeled using two flapwise mode shapes and one edgewise mode shape per blade. To manipulate blade structural response, the frequency of the flapwise and edgewise mode shapes was changed by $\pm 5\%$ of 0.7 Hz and 1 Hz, respectively, by uniformly scaling the associated stiffness. The blade mass was changed by uniformly scaling the distributed blade mass of all blades. The nominal scaling of 1.04536 is described in the NREL [5-MW-5-MW](#) specifications document (Jonkman et al., 2009). The blade CM location was changed by varying the blade root and tip density such that density increased at one end and decreased at the other without changing the overall blade mass. Blade imbalance effects were also included by varying the mode frequency and mass of each blade. The imbalances were introduced by applying a different change value to each blade. Specifically, one blade is modified to be a value that is higher than the nominal value, and another modified to a lower value. The third blade remains unchanged at the nominal value.

Table 8: Parameter value ranges of turbine blade structure parameter ranges.

| | B_{FK} (-) | B_{EK} (-) | $B_{FK,imb}$ (-) | $B_{EK,imb}$ (-) | B_{DR} (% _{critical}) | B_M (-) | $B_{M,imb}$ (-) | B_{CM} (m) | β_p (deg) |
|-------------|-----------------|-----------------|---------------------|---------------------|--------------------------------------|---------------|--------------------|-----------------|--------------------|
| Nom. | 1 | 1 | 0.01 | 0.01 | 1.55 | 1.04536 | 0.025 | 0.015 | -2.5 |
| Min. | 0.9 | 0.9 | 0.0 | 0.0 | 0.1 | 0.993 | 0.0 | 20.60 | -2.75 |
| Max. | 1.1 | 1.1 | 0.02 | 0.02 | 3.0 | 1.1 | 0.05 | 22.60 | -2.25 |
| Ref. | Exp | Exp | Exp | Exp | Exp | Witcher, 2017 | Exp | IEC, 2010 | Exp |

15 4.2.2.3 Blade Aerodynamic Properties

The blade aerodynamic properties were represented using 18 parameters: 3 associated with blade twist and chord distribution; 10 associated with the static aerodynamic component; and 5 associated with the unsteady aerodynamic properties. Blade twist and chord distributions were manipulated by specifying a change in the distributions along the blade. Three parameters were defined, associated with changing the chord at the blade tip and root, and the twist at the blade tip. For each of these parameters, the associated distribution along the blade was modified linearly such that there was zero change at the opposite end. The root twist was not changed because the blade-pitch angle uncertainties are considered in the controller parameter section.

4.2.2.4 Steady Airfoil Aerodynamics

For the steady aerodynamic component, the lift and drag versus angle-of-attack (AoA) curves were modified to examine the sensitivity on resulting loads throughout the wind turbine. The turbine operated in normal operating conditions, and therefore only relevant regions of the curves were modified. To modify the curves, the curves were parameterized using an approach based on one introduced by Abdallah et al. (2015). The approach used here parameterizes the C_l and C_d curves using five points; these points were perturbed and a spline fit to the points. The points of interest are:

- Beginning of linear C_l region — determines the lower limit of the AoA range of interest and was kept constant (α_{lin} , $C_{l,lin}$);
- C_d value at AoA = 0° (0° , $C_{d,0}$);
- Trailing edge separation (TES) point — AoA location at which C_l curve is no longer linear (α_{TES} , $C_{l,TES}$);
- Maximum (max) point — AoA location at which C_l reaches a maximum (α_{max} , $C_{l,max}$);
- Separation reattachment (SR) point — AoA location at which slope of C_l curve is no longer negative (α_{SR} , $C_{l,SR}$).

The selected points of interest are similar to those selected by Abdallah et al. (2015). A notable difference is the consideration of $C_{d,0}$ as opposed to $C_{d,90}$, which is the C_d value at $\alpha=90^\circ$. $C_{d,0}$ was chosen for this study because of the focus on normal

operational region, as opposed to the extreme conditions considered by Abdallah et al. (2015). The three variable points of interest were perturbed by a percentage of the default value. The perturbations and correlations are depicted in Figure 9-12 and parameter ranges are detailed in Table 9. From Abdallah (2015), the TES, max, and SR C_l values for an individual airfoil have a correlation to one another of 0.9. Thus, all C_l values are perturbed collectively, using the same percentage (δ_4). The AoA values are less correlated and are therefore perturbed independently of one another. However, to ensure that nonphysical

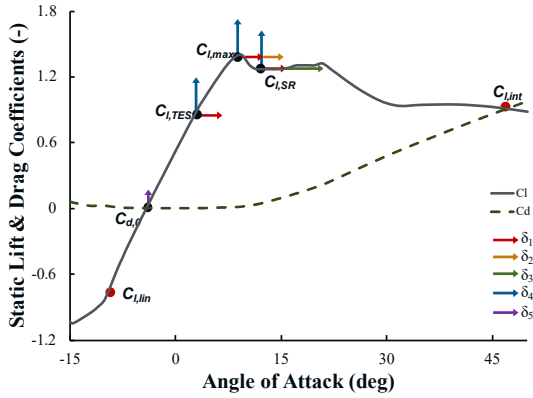


Figure 9: Perturbation of points of interest in representative C_l and C_d curves.

relative values are not reached, all AoA values are perturbed by the same base percentage (δ_1), and then an additional independent variation of a smaller value was added (δ_2 and δ_3) for α_{max} and α_{SR} , respectively. The $C_{d,0}$ value was also perturbed (δ_5).

10 C_l and C_d curves were altered for each airfoil. However, instead of specifying δ values for each airfoil, these values were specified at the root and tip airfoils, excluding the cylindrical airfoils at the base. Perturbation values for the interior airfoils were computed from a linear fit of the endpoint values. The method of developing the new curves for each airfoil is detailed here:

1. AoA deltas are applied to the original AoA values via the following equations:

$$\alpha_{TES,new} = \alpha_{TES,orig} + \alpha_{TES,orig} \delta_1 \quad (8)$$

$$\alpha_{max,new} = \alpha_{max,orig} + \alpha_{max,orig} (\delta_1 + \delta_2) \quad (9)$$

$$\alpha_{SR,new} = \alpha_{SR,orig} + \alpha_{SR,orig} (\delta_1 + \delta_3) \quad (10)$$

- 15 2. The new AoA values are fit to the nearest existing AoA value on the curve. The AoA resolution is fine enough that all perturbations are captured, though not precisely. This approach may need to be adjusted if the perturbations were to decrease.
3. For all new AoA values, the change in C_l between the original C_l value ($C_{l,orig}$) and the C_l curve value at the new AoA ($C_{l,orig+}$) is computed via:

$$\epsilon = C_{l,orig+} - C_{l,orig}$$

20

4. The total change in C_l is then computed via:

$$C_{l,diff} = \delta_4 C_{l,orig} - \epsilon$$

This ensures that if $\delta_i = 0$, the final $C_{l,new}$ value is equivalent to that of the original curve.

5. For C_l perturbation, the end points are located at the AoA associated with the beginning of the linear C_l region ($C_{l,lin}$) and $\alpha = 90^\circ$; as these are fixed points, they have $C_{l,diff} = 0$. The C_l curve is replaced by a line between $(\alpha_{lin}, C_{l,lin})$ and $(\alpha_{TES}, \delta_4 C_{l,lin})$. A piece-wise linear spline – representing perturbations about the original curve – is constructed between the points $(\alpha_{TES,new}, \delta_4 C_{l,TES})$; $(\alpha_{max,new}, \delta_4 C_{l,max})$; $(\alpha_{SR,new}, \delta_4 C_{l,SR})$; and $(90^\circ, 0)$.
6. The $C_{l,diff}$ values calculated from the spline fit are added to the original C_l curve.

$$C_{l,new} = C_{l,orig} + C_{l,diff}$$

A similar process was followed by modifying the C_d curves, wherein the C_d value corresponding to $\alpha = 0^\circ$ ($C_{d,0}$) is perturbed by a specified value (δ_5) in the same manner as the C_l values. A piece-wise linear spline is then fit between $(-90^\circ, C_{d,-90})$, $(0^\circ, C_{d,0})$, and $(90^\circ, C_{d,90})$ and added to the original C_d curve. $C_{d,0}$ is constrained to not go below 0. Several modified C_l and C_d curves for each airfoil section are shown in Figure 10. Note that C_d curves are perturbed, but by a very small amount not visible in the plots. These perturbations result in modified C_l and C_d curves that maintain the primary characteristics of the original curve, but differ in both magnitude and feature location.

4.2.2.5 Unsteady Airfoil Aerodynamics

There are several unsteady airfoil aerodynamic parameters that can be modified in OpenFAST. By expert opinion (Damiani, 2018), several of these parameters have been identified as having the largest potential variability or impact on turbine response and are therefore included in this study. Several of the parameters in the Beddoes-Leishman-type unsteady airfoil aerodynamics model used here are derivable from the (perturbed) static lift and drag polars (i.e., when the lift and drag polars are perturbed, the associated Beddoes-Leishman unsteady airfoil aerodynamic parameters are perturbed as well). Additionally, there are several other parameters associated with unsteady aerodynamics that are included in OpenFAST. These parameters are:

- T_{f0} — time constant connected to leading-edge separation of the airfoil;
- T_{V0} — time constant connected to vortex shedding;
- T_p — time constant connected to the leading-edge pressure gradient;
- T_{VL} — time constant connected to the vortex advection process;
- St_{sh} — Strouhal number associated with the vortex shedding frequency.

These quantities were varied over the ranges detailed in Table 9 and are constant across the blade.

Table 9: Parameter value ranges of turbine blade aerodynamic parameter ranges.

| | θ_{tip} (deg) | c_r (m) | c_t (m) | T_{f0} (-) | T_{V0} (-) | T_p (-) | T_{VL} (-) | St_{sh} (-) | $C_{l,tr}$ (-) | $\alpha_{TES,tr}$ (deg) | $\alpha_{max,tr}$ (deg) | $\alpha_{SR,tr}$ (deg) | $C_{d,0,tr}$ (-) |
|-------------|-------------------------|-----------------------|-----------------------|----------------------|----------------------|----------------------|----------------------|----------------------|-----------------------|----------------------------|----------------------------|---------------------------|----------------------|
| Nom. | 0.106 | 3.542 | 1.419 | 6.5 | 8 | 1.35 | 16.5 | 0.245 | Var. | Var. | Var. | Var. | Var. |
| Min. | -1.894 | 3.1878 | 1.2771 | 3 | 1 | 1 | 11 | 0.19 | -26% | -20% | -8% | -15% | -100% |
| Max. | 2.106 | 3.8962 | 1.5609 | 10 | 15 | 1.7 | 22 | 0.3 | +26% | +20% | +8% | +15% | +100% |
| Ref. | Petrone et al., 2011 | Loeven and Bijl, 2008 | Loeven and Bijl, 2008 | Damiani et al., 2016 | Damiani et al., 2016 | Damiani et al., 2016 | Damiani et al., 2016 | Damiani et al., 2016 | Abdallah et al., 2015 | Abdallah et al., 2015 | Abdallah et al., 2015 | Abdallah et al., 2015 | Ehrmann et al., 2017 |

Formatted: Font: Not Italic

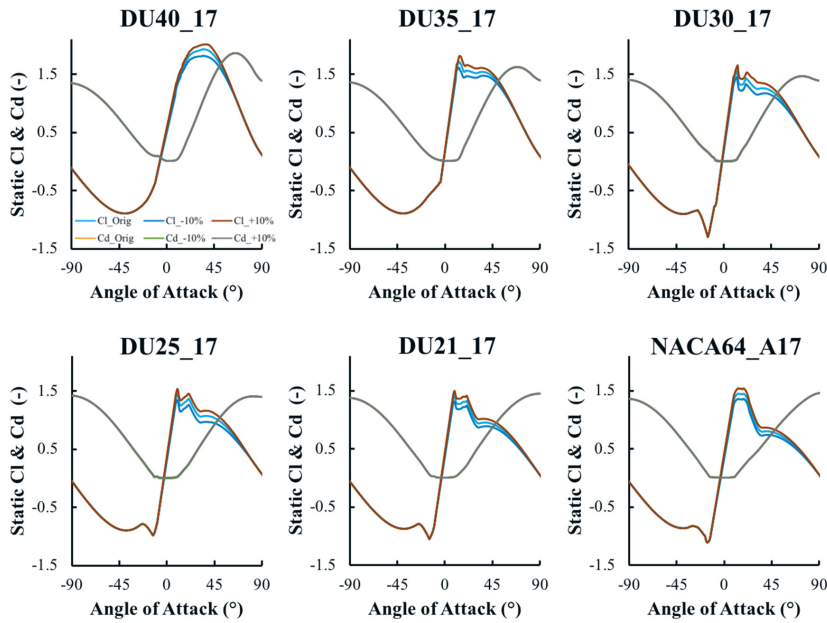


Figure 10: Sample original and perturbed C_l and C_d curves for each airfoil section used in the NREL 5MW5-MW reference turbine. Perturbed values represent $\pm 10\%$ of the specified range for each parameter.

5 4.2.2.6 Controller Properties

Turbine yaw error was incorporated by directly changing the yaw angle of the turbine. For the collective blade pitch error, the twist distribution of each blade is identically shifted uniformly along the blade independent of the twist change in Table 9. For the imbalance pitch error, modified twist distributions are applied to two of the blades: one with a higher-than-nominal tip twist, one with a lower-than-nominal tip twist, and one unchanged.

10

Table 10: Parameter value ranges of turbine controller parameter ranges.

| | θ (deg) | $\theta_{err, coll}$ (deg) | $\theta_{err, imb}$ (deg) |
|-------------|--------------------|-------------------------------|------------------------------|
| Nom. | 0 | 0 | 0.1 |
| Min. | -20 | -0.2 | 0 |
| Max. | 20 | 0.2 | 0.2 |
| Ref. | Quick et al., 2017 | Simms et al., 2001 | Simms et al., 2001 |

4.3 Elementary Effects

The EE value calculation and analysis process are the same as was used for the wind parameter analysis. 60 wind file seeds were needed based on a convergence study of the ultimate and fatigue load metrics for all QoIs. This increase in the number in required wind file seeds over the other study is likely due to some turbine input parameter combinations causing resonance.

5 Based on these numbers, the total number of simulations performed for the wind-inflow case study was $R \times (I+1) \times S \times B = 30 \times 40 \times 60 \times 3 = 216,000$.

The EE values across all input parameters, input hyperspace points, and wind speed bins were examined for all QoI for the ultimate and fatigue loads. For each QoI, the number of times an EE value exceeded the threshold for a given QoI was tallied.

10 The resulting tallies are shown in Figure 11, with the ultimate load tally on the top and fatigue load tally on the bottom. Note that nearly twice as many significant events were counted for fatigue loads; less significant events were counted for ultimate loads because of the limited threshold exceedance in the below-rated wind speeds. The percentage that each relevant input parameter contributed to the total significant event count is summarized in Table 11. Ultimate turbine loads are most sensitive to yaw error (θ) and C_1 distribution at the outboard section of the blade ($C_{1,o}$), which combined accounted for nearly half of all significant events. Fatigue loads are also highly sensitive to blade mass imbalance ($B_{M,imb}$). Turbine loads are also sensitive to twist distribution (ϕ), blade mass (B_M), and the C_1 distribution at the inboard section of the blade ($C_{1,i}$). Though these results are expected, their [relevant-relative](#) importance is likely a new finding. Other input parameters that were found to affect turbine load sensitivity are inboard maximum AoA ($\alpha_{max,b}$), blade mass center of mass (B_{CM}), blade flapwise stiffness (B_{FK}), nacelle center of mass location (N_{CM}), nacelle mass (N_{mass}), chord length at the inboard section of the blade (c_b), tower stiffness (T_{KF}), drivetrain damping (D_D), and inboard trailing edge separation AoA ($\alpha_{TES,b}$). The AoA values at the inboard section of the blade are likely more important than at the outboard section due to the higher likelihood of the inboard section operating with higher AoA near stall. Additionally, the range of AoA values at the inboard section is larger than at the outboard section because the nominal inboard AoA values are higher, which could contribute to greater sensitivity.

15

20

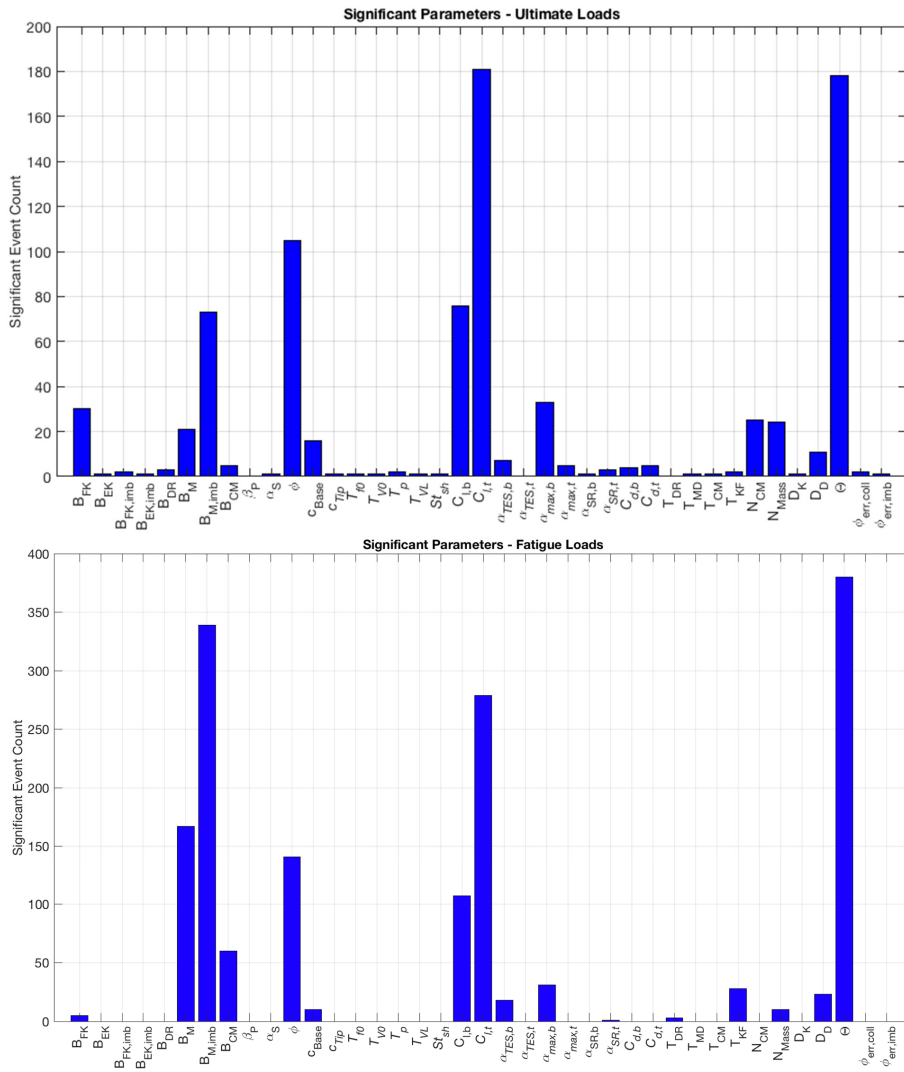


Figure 11: Identification of significant parameters using ultimate (top) and fatigue loads (bottom). Significant events are defined by the number of outliers identified across each of the QoIs for all wind speed bins, input parameters, and simulation points.

Table 11. Percentage of contribution to total number of significant events for ultimate and fatigue loads.

| | θ (deg) | $B_{M,imb}$ (-) | C_{lt} (-) | ϕ (deg) | B_M (-) | C_{lb} (-) | $\alpha_{max,b}$ (deg) | B_{CM} (-) | B_{FK} (-) | N_{CM} (m) | N_{mass} (kg) | $\alpha_{TES,b}$ (deg) | c_b (m) | T_{KF} (m) | D_D (m) |
|---------------|-------------------|--------------------|-----------------|-----------------|--------------|-----------------|---------------------------|-----------------|-----------------|-----------------|--------------------|---------------------------|--------------|-----------------|--------------|
| Ult. Load (%) | 21.5 | 8.8 | 21.9 | 12.7 | 2.5 | 9.2 | 4.0 | 0.6 | 3.6 | 3.0 | 2.9 | 0.8 | 1.9 | 0.2 | 1.3 |
| Fat. Load (%) | 23.7 | 21.2 | 17.4 | 8.8 | 10.4 | 6.7 | 1.9 | 3.7 | 0.3 | 0.0 | 0.6 | 1.9 | 0.6 | 1.7 | 1.4 |

Histograms of the EE values for each of the QoIs are plotted in Figure 12 - Figure 15 for the ultimate and fatigue load metrics (associated exceedance probability plots are shown in Appendix B, Figure 23, Figure 21, and Figure 24). Here, EE values are colored by wind speed and the black vertical line represents the threshold for each QoI. The sharp separation of ultimate load EE values between wind speed bins is evident in Figure 12. A zoomed-in view of the lower count values is shown in Figure 13. The more evenly distributed nature of the fatigue load EE values is further highlighted in the histogram plots depicted in Figure 14 and zoomed in Figure 15. Unlike ultimate load EE values, all wind speed bins contribute to the outlier count for each QoI. Histogram plots of blade-root ultimate and fatigue bending moment EE values are shown in Figure 16 and Figure 17, respectively. The sharp separation of ultimate load EE values between wind speed bins is again evident. Highlighted in the fatigue load plots is the more even distribution of threshold-exceeding EE values across wind speed bins.

Exceedance probability of the EE values for all QoIs are plotted in Figure 15 and Figure 16 for the ultimate and fatigue load metrics, respectively. The figures were prepared in the same manner as Figure 5 and Figure 6. As shown in Figure 15, ultimate load EE values are largely grouped by wind speed bin for all QoIs with the exception of blade-root pitching moment. These grouping of the results by wind speed bin results highlight the creates an unequal distribution of outliers resulting from each turbine QoI. Most notably, blade-root pitching moment accounts for 18% of the total ultimate load significant events, whereas rotor torque accounts for only 5%. This suggests that it may be better to tailor the threshold for each QoI, but this was deemed overly complicated for this first pass at assessing the sensitivity. Additionally, for a given QoI, it is typical for all ultimate load significant events to occur from either the near- or above-rated wind speeds. However, fatigue load EE values are more evenly distributed across wind speed bins, as shown in Figure 14, Figure 16. The lower significant event counts for ultimate loads is a result of the segregated nature of the ultimate load EE values, as opposed to the more evenly distributed nature of the fatigue load EE values. In fact, unlike ultimate load EE values, a large percentage of significant events result from below-rated wind speed cases because of the higher probability of low wind speed conditions. However, the distribution of fatigue load outliers resulting from each turbine QoI is approximately the same as the distribution for ultimate load outliers, with 14.6% of outliers resulting from the blade-root OoP bending moment and only 4.3% resulting from the blade-root pitching moment. Note that the QoI (blade-root pitching moment) that contributed the most outliers for ultimate load outliers contributes the least for fatigue load outliers.

These points are further highlighted by computing EE value histograms for ultimate and fatigue load QoIs. Ultimate load histograms are shown in Figure 17. Here, EE values are again colored by wind speed and the black vertical line represents the threshold for each QoI. The sharp separation of ultimate load EE values between wind speed bins is again evident. A zoomed-in view of the lower count values is shown in Figure 18. These plots highlight the separation of wind speed bin EE values. The more evenly distributed nature of the fatigue load EE values is further highlighted in the histogram plots depicted in Figure 19 and zoomed in Figure 20. Unlike ultimate load EE values, all wind speed bins contribute to the outlier count for each QoI. Histogram plots of blade-root ultimate and fatigue bending moment EE values are shown in Figure 21 and Figure 22, respectively. The sharp separation of ultimate load EE values between wind speed bins is again evident. Highlighted in the fatigue load plots is the more even distribution of threshold-exceeding EE values across wind speed bins.

Field Code Changed

Field Code Changed

Field Code Changed

Field Code Changed

Formatted: Font color: Auto

Field Code Changed

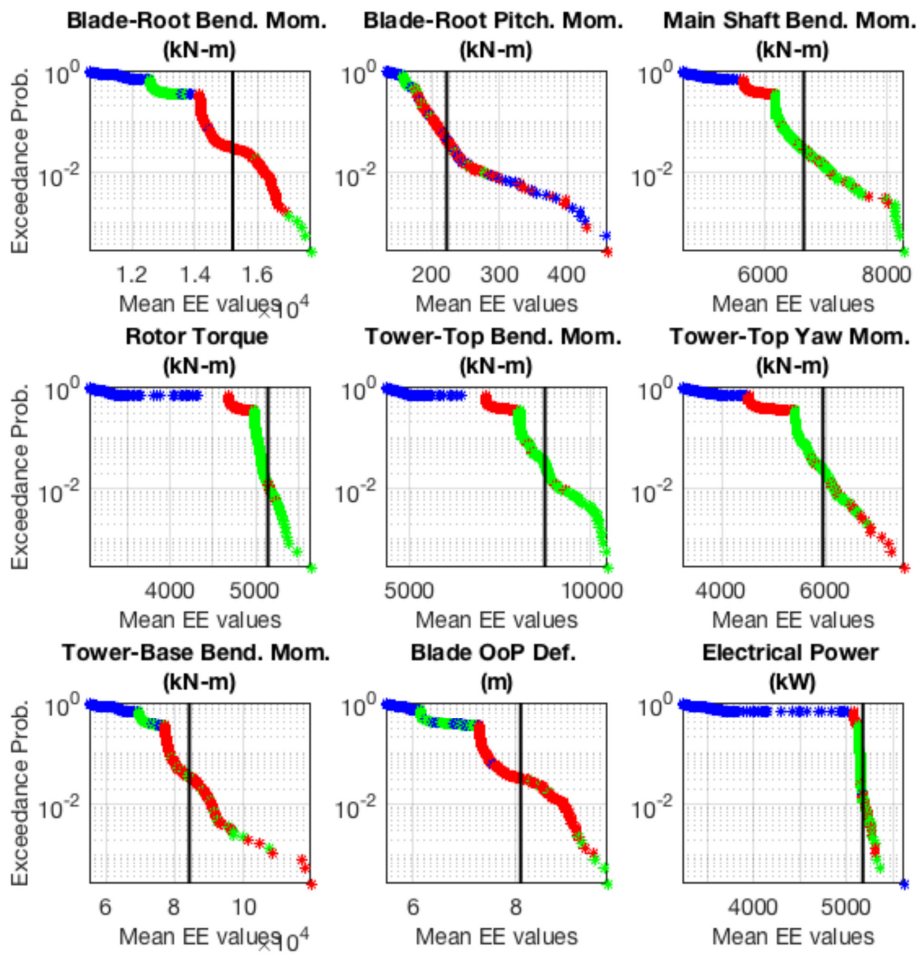


Figure 15: EE-value exceedance probability plots of ultimate loads across all wind speed bins, input parameters, and simulation points for all QoIs. The black line represents the defined threshold by which outliers are counted for each QoI. Color indicates wind speed bin (blue=below rated, red=near rated, green=above rated).

Formatted: Justified

Formatted: Normal

Formatted: Justified, Don't keep with next

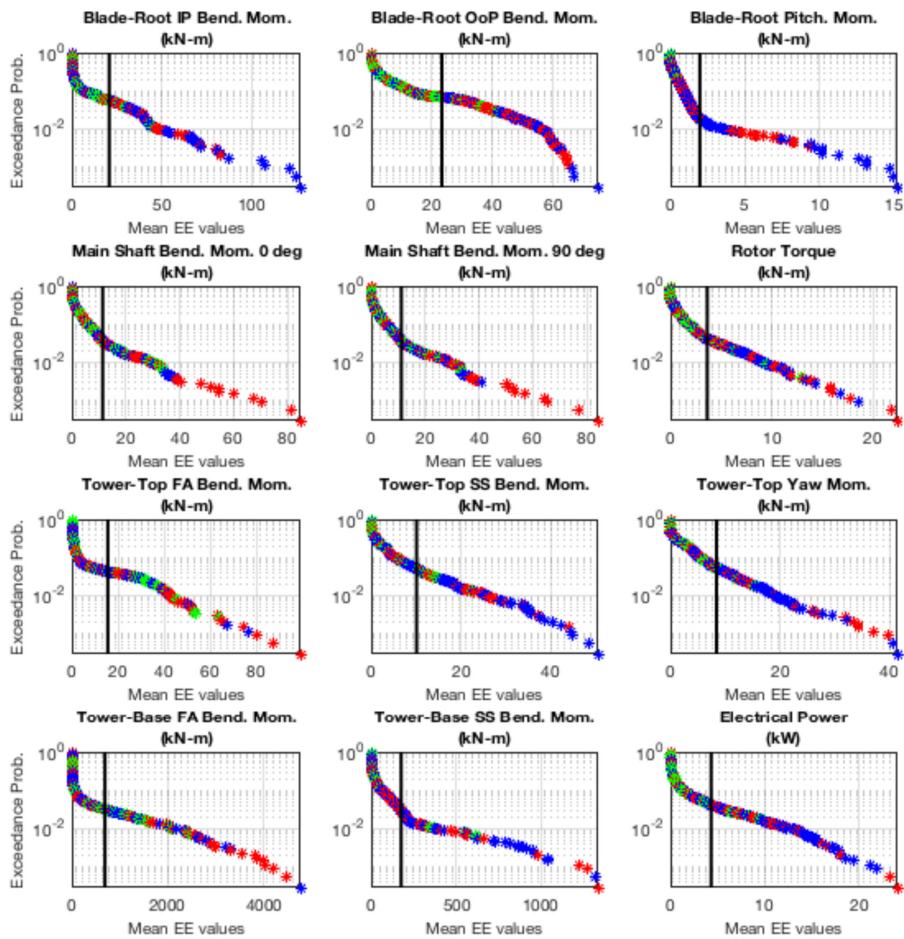


Figure 16: EE value exceedance probability plots of fatigue loads across all wind speed bins, input parameters, and simulation points for all QoIs. The black line represents the defined threshold by which outliers are counted for each QoI. Color indicates wind speed bin (blue=below rated, red=near rated, green=above rated).

Formatted: Normal

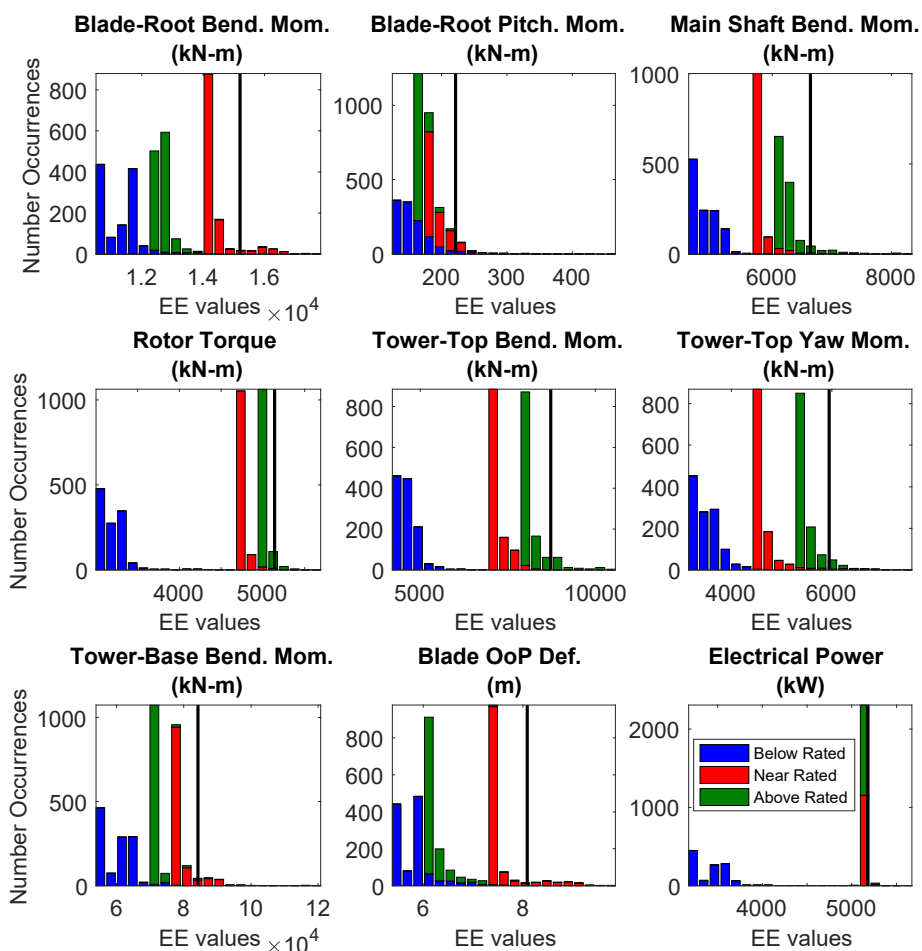


Figure 12: Stacked EE-values histograms of ultimate loads across all wind speed bins, input parameters, and simulation points for all QoIs. The black line represents the threshold by which outliers are counted for each QoI. Color indicates wind speed bin (blue=below rated, red=near rated, green=above rated).

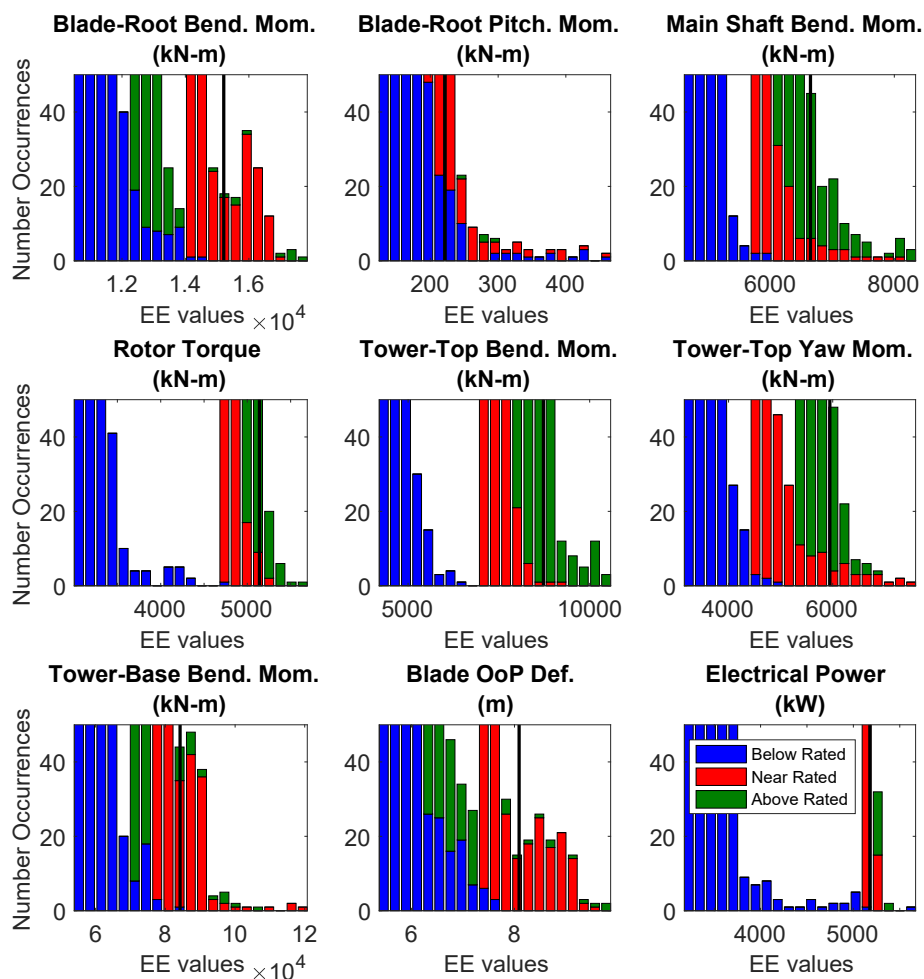


Figure 13: Zoomed-in stacked EE-values histograms of ultimate loads across all wind speed bins, input parameters, and simulation points for all QoIs. The black line represents the threshold by which outliers are counted for each QoI. Color indicates wind speed bin (blue=below rated, red=near rated, green=above rated).

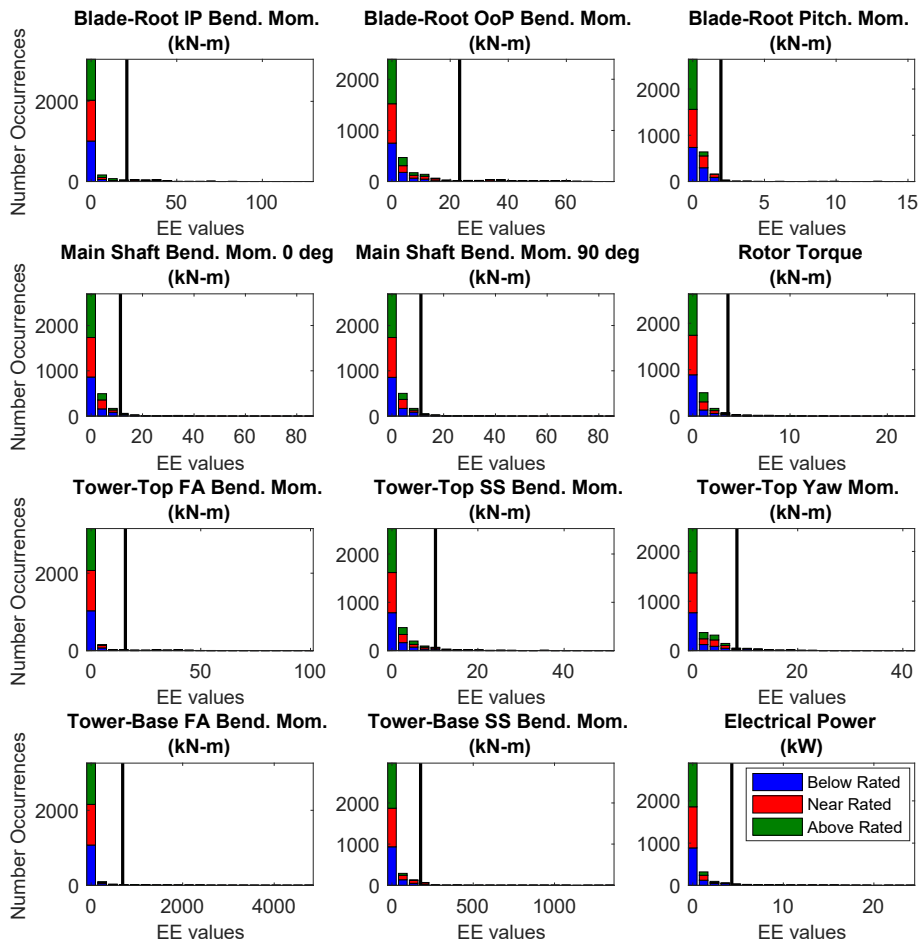


Figure 14: Stacked EE-values histograms of fatigue loads across all wind speed bins, input parameters, and simulation points for all QoIs. The black line represents the threshold by which outliers are counted for each QoI. Color indicates wind speed bin (blue=below rated, red=near rated, green=above rated).

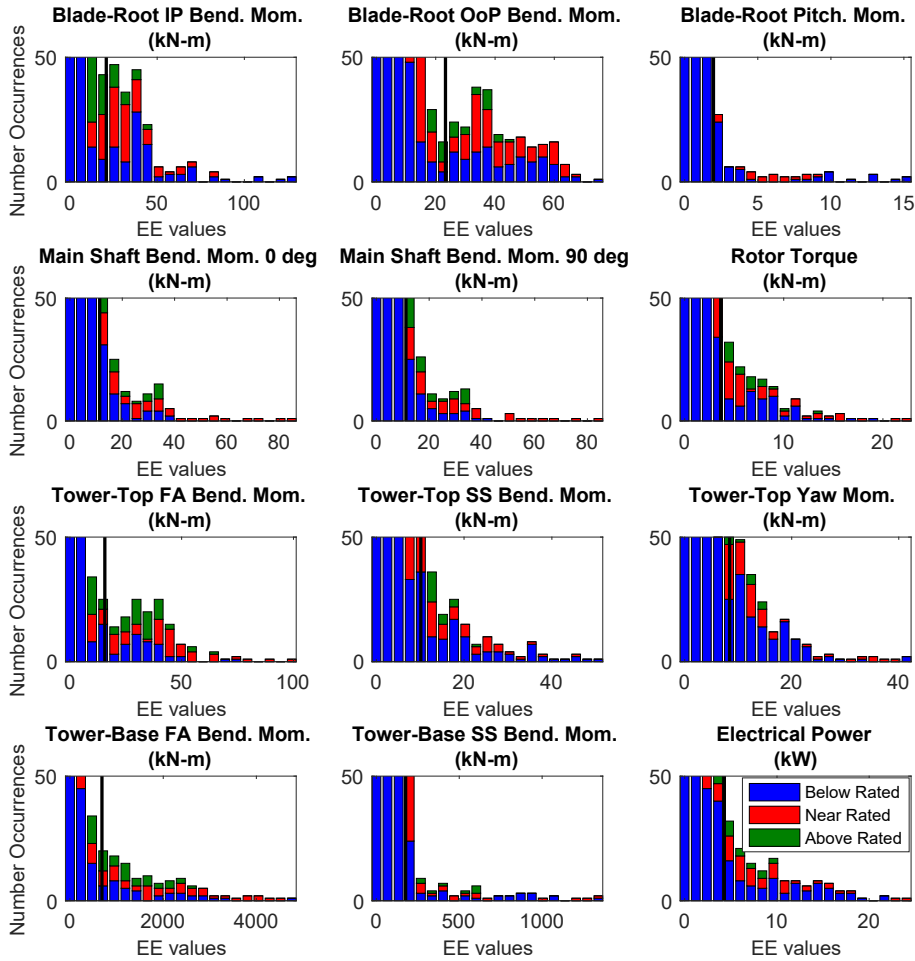


Figure 15: Zoomed-in stacked EE-values histograms of fatigue loads across all wind speed bins, input parameters, and simulation points for all QoIs. The black line represents the threshold by which outliers are counted for each QoI. Color indicates wind speed bin (blue=below rated, red=near rated, green=above rated).

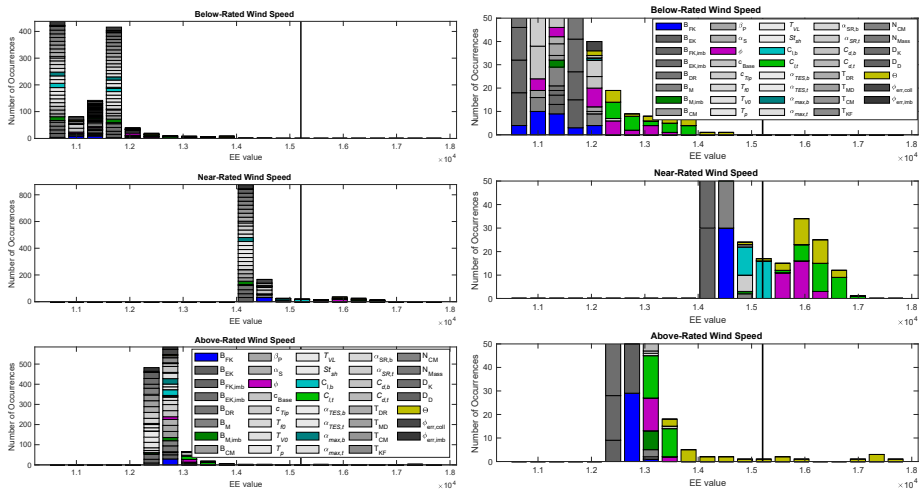


Figure 16: EE-values histograms of blade-root bending ultimate moment. Each graph shows one wind speed bin and includes all input parameters. Right column is a zoomed-in view of the left column.

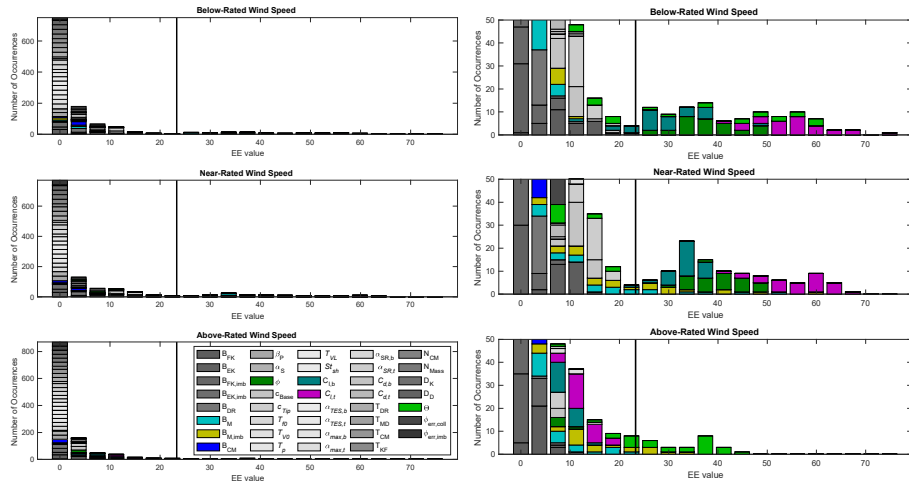


Figure 17: EE-value histograms of blade-root OoP bending fatigue moment. Each graph shows one wind speed bin and includes all input parameters. Right column is a zoomed-in view of the left column.

5

The behavior of blade-root loads are examined in more detail by plotting exceedance probability distinctly for each input parameter in Figure 18. Highlighted in these plots is the contribution of the individual input parameters to the outlier counts. For blade-root bending ultimate moment EE values, blade twist and $C_{1,t}$ EE values in the near-rated wind speed bin are beyond the threshold for every point in the hyperspace. Yaw error and $C_{1,b}$ EE values from the near-rated wind speed bin and yaw error from the above-rated wind speed bin also cross the threshold. For blade-root OoP bending fatigue moment EE values, the threshold is exceeded by blade twist and $C_{1,t}$ EE values from the below- and above-rated wind speeds for every point in the hyperspace. However, for all other relevant input parameters, only certain points in the hyperspace result in threshold exceedance. This indicates that, for certain loads and input parameters, the sensitivity of the turbine is dependent on the combination of turbine parameter values. These results can be used in future studies to more thoroughly investigate the hyperspace to determine how input parameter value combinations contribute to turbine sensitivity.

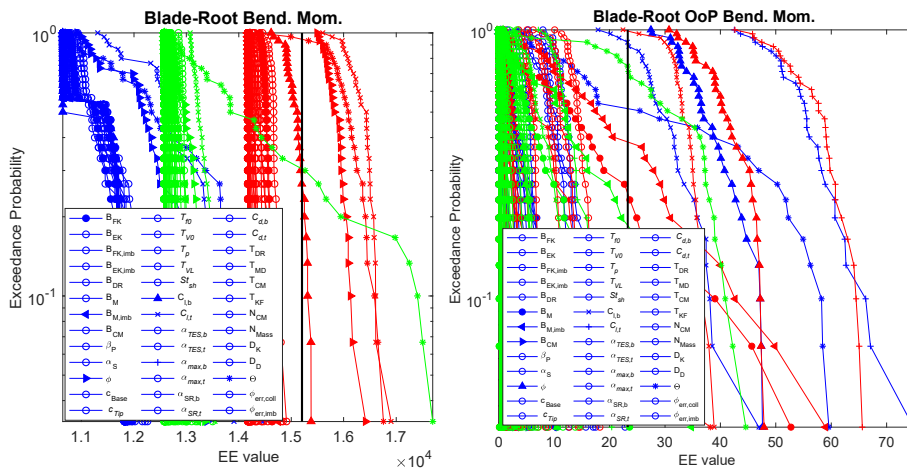


Figure 18: EE-value exceedance probability plots for the blade-root bending ultimate moment (left) and blade-root OoP bending fatigue moment (right). Each line represents a different input parameter and wind speed bin (blue=below rated, red=near rated, green=above rated).

For each QoI, the number of times each input parameter contributed to the significant event count was tallied. The top parameters are shown in Table 10-12 and Table 11-13 for ultimate and fatigue loads, respectively. Overall, 63% of the top sensitive parameters for both ultimate and fatigue loads are due to aerodynamic perturbations or yaw error. Blade-root and main shaft moments are especially sensitive to perturbations of inputs. However, blade mass imbalance and blade mass account for 44% of the most sensitive parameters associated with tower moment fatigue loads. Rotor torque ultimate and fatigue loads are most sensitive to perturbation of structural input parameters, especially those related to blade mass. For both ultimate and fatigue loads, electrical power is most sensitive to blade mass imbalance, blade mass factor, and yaw error. These results can be used in future sensitivity analysis work to focus on perturbation of specific input parameters based on desired turbine loads.

Table 12. Top input parameters contributing to ultimate load sensitivity of each QoI. Values indicate how many times the variable contributes to the sensitivity count.

| Blade-Root Bend. Mom. | Blade-Root Pitch. Mom. | Main Shaft Bend. Mom. | Rotor Torque | Tower-Top Bend. Mom. | Tower-Top Yaw Mom. | Tower-Base Bend. Mom. | Blade OoP Deflection |
|-----------------------|------------------------|-----------------------|------------------|----------------------|--------------------|-----------------------|----------------------|
| θ (39) | $\alpha_{max,b}$ (33) | θ (43) | $B_{M,imb}$ (26) | θ (28) | $C_{1,t}$ (28) | $\phi C_{1,t}$ (30) | $\phi C_{1,b}$ (30) |

| | | | | | | | |
|---------------------|----------------|----------------|------------|-----------------------|----------------|------------------|---------------|
| $\phi/C_{1,t}$ (30) | $C_{1,b}$ (15) | $C_{1,t}$ (37) | D_D (25) | N_M (19) | θ (25) | $C_{1,b}$ (28) | B_{FK} (28) |
| $C_{1,b}$ (7) | ϕ (14) | c_b (22) | B_M (17) | $N_{CM}/C_{1,t}$ (17) | $C_{1,b}$ (21) | $B_{M,imb}$ (27) | θ (27) |

Table 13. Top input parameters contributing to fatigue load sensitivity of each QoI. Values indicate how many times the variable contributes to the sensitivity count.

| Blade-Root IP Bend. Moment | Blade-Root OP Pitch. Moment | Blade-Root Pitch. Moment | Main Shaft Bending Moment 0° | Main Shaft Bending Moment 90° | Rotor Torque | Tower-Top FA Bend. Moment | Tower-Top SS Bend. Moment | Tower-Top Yaw Moment | Tower-Base FA Bend. Moment | Tower-Base SS Bend. Moment |
|----------------------------|-----------------------------|--------------------------|------------------------------|-------------------------------|------------------|---------------------------|---------------------------|----------------------|----------------------------|----------------------------|
| B_{CM} (59) | $\phi/C_{1,t}$ (60) | $\alpha_{max,b}$ (31) | θ (49) | θ (49) | $B_{M,imb}$ (51) | θ (75) | θ (64) | $C_{1,t}$ (59) | $B_{M,imb}$ (59) | T_{KF} (28) |
| $B_{M,imb}$ (52) | $C_{1,b}$ (54) | $\alpha_{RES,b}$ (18) | $C_{1,t}$ (44) | $C_{1,t}$ (42) | θ (31) | $B_{M,imb}$ (54) | $C_{1,t}$ (52) | $B_{M,imb}$ (42) | B_M (48) | $B_{M,imb}$ (26) |
| B_M (47) | θ (36) | c_b (11) | ϕ (16) | ϕ (19) | B_M (28) | B_M (21) | $B_{M,imb}$ (38) | θ/ϕ (27) | T_{DR} (2) | $B_M/C_{1,t}/N_M$ (10) |

Formatted: Font: Not Italic

Formatted: Font: Not Italic

Conclusions

- 5 A screening analysis of the most sensitive turbulent wind and aeroelastic parameters to the resulting structural loads and power output-QoI was performed for the representative NREL 5-MW5-MW wind turbine under normal operating conditions. The purpose of the study was to assess the sensitivity of different turbulent wind and turbine parameters on the resulting loads of the wind turbine. The sensitivities of the different parameters were ranked. The study did not consider specific site conditions, but rather focused on understanding the most sensitive parameters across the range of possible values for a variety of sites.
- 10 To limit the number of simulations required, a screening analysis using the EE method was used instead of a more computationally intensive sensitivity analysis. The EE method is an assessment of the local sensitivity of a parameter at a given location in space through variation of only that parameter, examined over multiple points throughout the parameter hyperspace, making it a global sensitivity analysis. This work modified the general EE formula to examine the sensitivity of parameters across multiple wind speed bins. A radial version of the method was employed, using Sobol numbers as starting points, and a set delta value of 10% for the parameter variations.
- 15 Two independent case studies were performed. For the wind parameter case study, it was found that the loads and power are highly sensitive to the shear and turbulence levels in the u-direction. To a lesser extent, turbine loads are sensitive to the wind veer and the integral length scale and coherence parameters in the u-direction. The combinations of parameters in this study spanned the ranges of several different locations. The parameters were considered independent of one another (conditioned only on wind speed bin), which likely resulted in some non-physical wind scenarios. However, the screening analysis has shown which parameters are most important to examine in more detail in future work.
- 20 The aeroelastic parameter case study showed that the loads and power are highly sensitive to the yaw error and the lift distribution at the outboard section of the blade. To a lesser extent, turbine loads are sensitive to blade twist distribution, lift distribution at the inboard section of the blade, and blade mass factor imbalance. Additionally, ultimate load EE values are typically separated by wind speed bin, whereas fatigue load EE values are more evenly distributed across wind speed bins.
- 25 Through the implemented EE method, different combinations of input parameters have been used. When specific input parameters are shown to be sensitive to one or more turbine loads, it is possible that only certain combinations of the input parameters will result in this sensitivity. This leads to opportunities for future work to further investigate which parameter combinations lead to higher turbine sensitivity. In future work, this ranking of most-sensitive parameters could be used to help establish error bars around predictions of engineering models during validation efforts and provide insight into probabilistic design methods and site-suitability analysis. While the most-sensitive ranking results may depend on the turbine size or
- 30
- 35

configuration, the analysis process developed here could be applied universally to other turbines. This work could also be further expanded in future work to include load cases other than normal operation.

Appendix A – Mean and Standard Deviation of Elementary Effects

To identify which parameters are the most sensitive, some researchers compare the average of the EE values for the different parameters across all input starting points. Additionally, some look at the standard deviation of the EE values for a given parameter across the different starting points. This helps to identify large sensitivity variation at different points, indicating strong interaction with the values of other parameters. As commonly found in EE-related literature, EE analysis typically identifies the most sensitive parameters using a plot to pictorially show the standard deviation versus mean values of the EE values. However, it is difficult to systematically identify the most sensitive parameters using this approach.

The mean of the absolute EE value for the ultimate loads for each QoI with input parameter i , and bin b is calculated as:

$$\mu_{\epsilon_{ib}}^* = \frac{1}{R} \sum_{r=1}^R |EE_{\epsilon_{ib}}^r| \quad (11)$$

where R is the number of points at which the EE value is calculated. The standard deviation of the EE is then calculated as:

$$\sigma_{\epsilon_{ib}} = \sqrt{\frac{1}{(R-1)} \sum_{r=1}^R (EE_{\epsilon_{ib}}^r - \mu_{\epsilon_{ib}})^2} \quad (12)$$

and $\mu_{\epsilon_{ib}}$ is defined as:

$$\mu_{\epsilon_{ib}} = \frac{1}{R} \sum_{r=1}^R EE_{\epsilon_{ib}}^r \quad (13)$$

This is shown in Figure 19 and Figure 20 for the blade-root bending ultimate moment and the blade-root bending OoP fatigue moment metrics for both the wind parameter and turbine parameter case studies, respectively. Shown in Figure 19 is the large sensitivity of shear in the lowest wind speed bin and the large sensitivity of the u-turbulence across all wind speed bins. Shown in Figure 20 is the large sensitivity of yaw error in the below-rated wind speed bin and the large sensitivity of the lift distribution at the outboard section of the blade in the below- and near-rated wind speed bins.

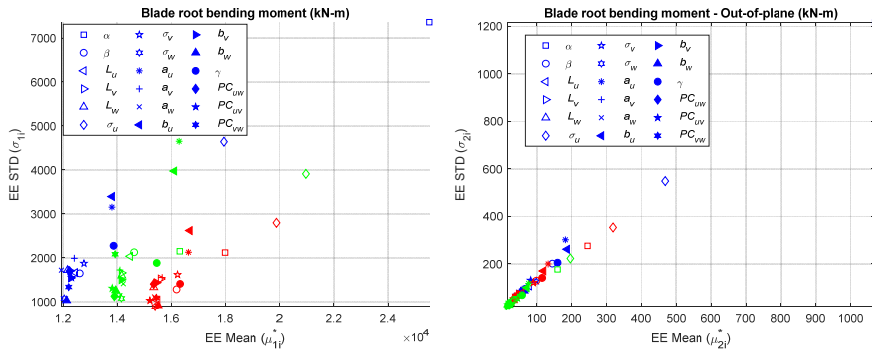


Figure 19: EE standard deviation vs EE mean for blade-root bending moment ultimate load (left) and blade-root out-of-plane bending moment fatigue load (right) at all wind speed bins (blue=below rated, red=near rated, green=above rated).

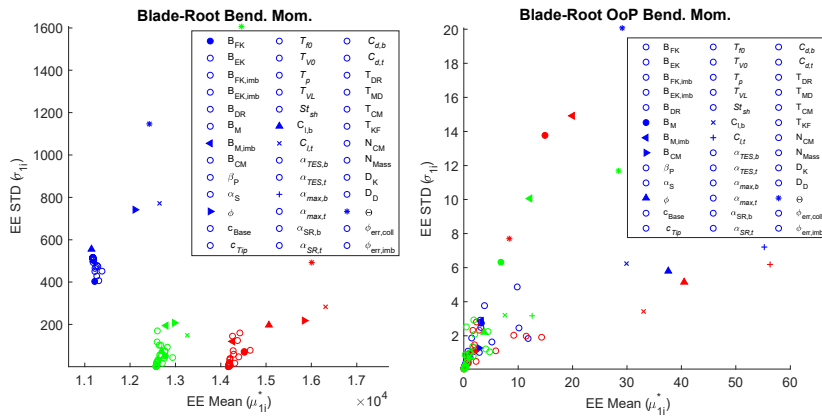


Figure 20: EE standard deviation vs EE mean for blade-root bending moment ultimate load (left) and blade-root out-of-plane bending moment fatigue load (right) at all wind speed bins (blue=below rated, red=near rated, green=above rated).

Appendix B – Exceedance Probability Plots of Elementary Effects

Formatted: Heading 1

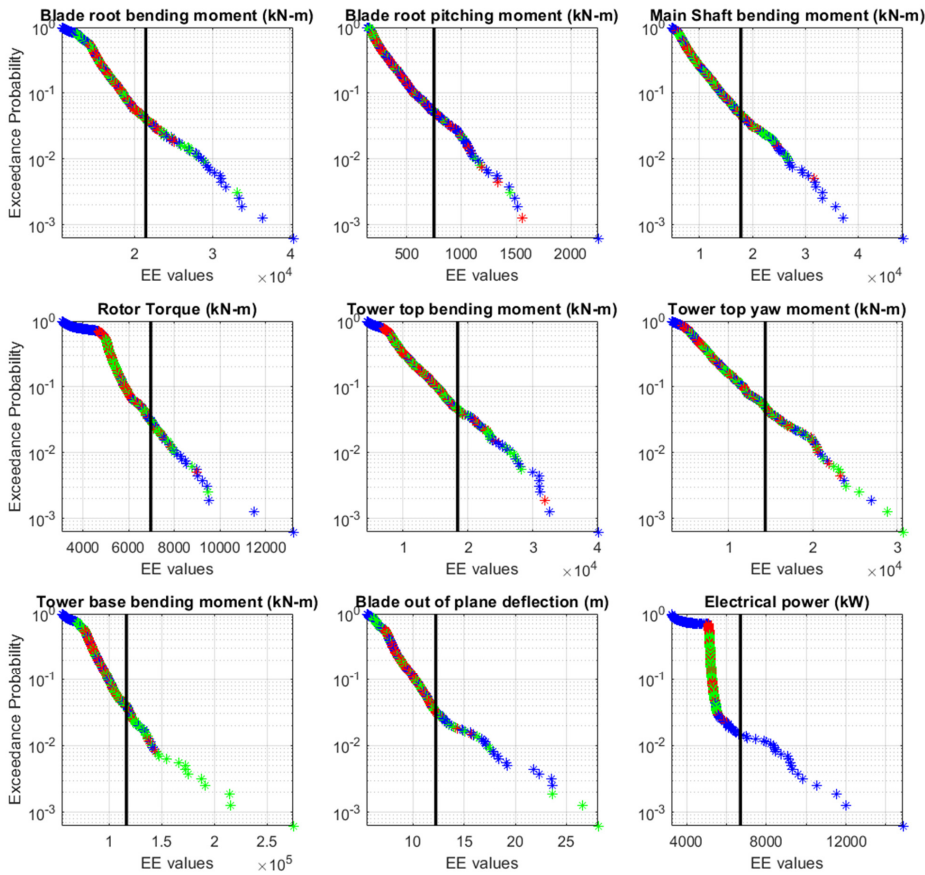


Figure 21: Exceedance probability plot of ultimate load EE values for each of the wind-inflow parameter QoIs across all wind speed bins, input parameters, and simulation points. Black line represents the defined threshold by which outliers are counted for each QoI. Color indicates wind speed bin (blue=below rated, red=near rated, green=above rated).

5

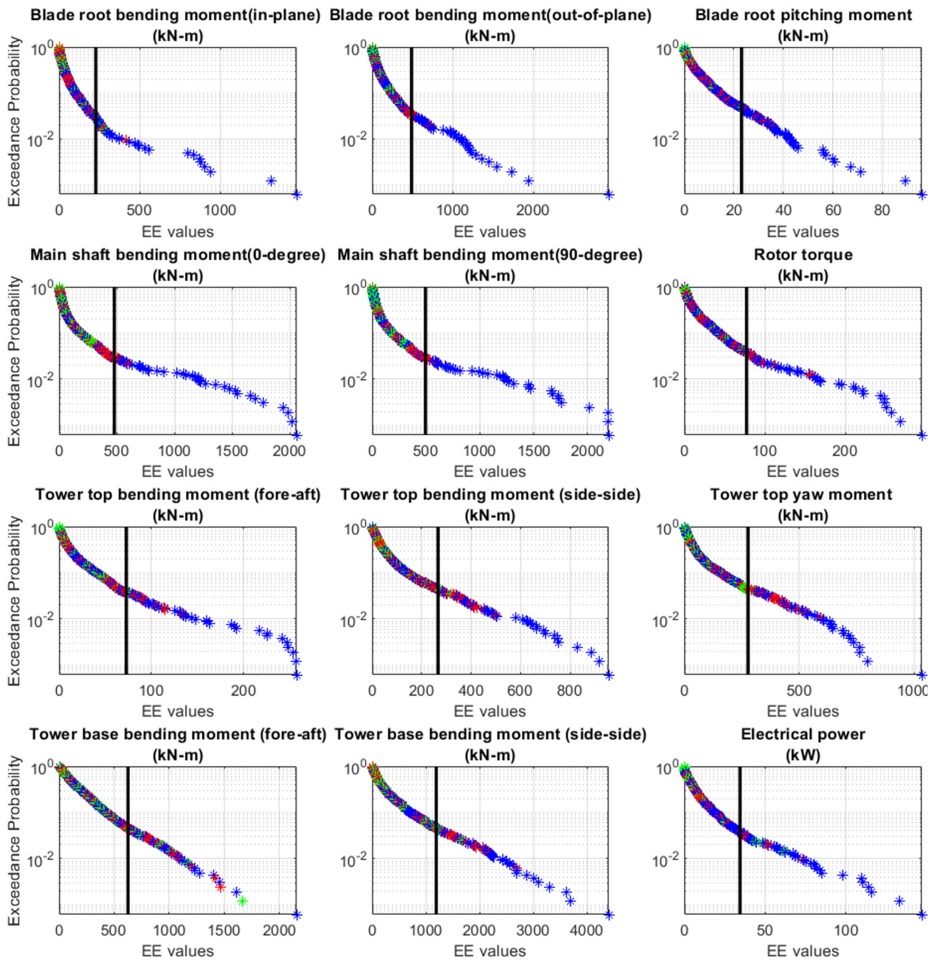


Figure 22: Exceedance probability plot of fatigue load EE values for each of the wind-inflow parameters across all wind speed bins, input parameters, and simulation points. Black line represents the defined threshold by which outliers are counted for each OoL. Color indicates wind speed bin (blue=below rated, red=near rated, green=above rated).

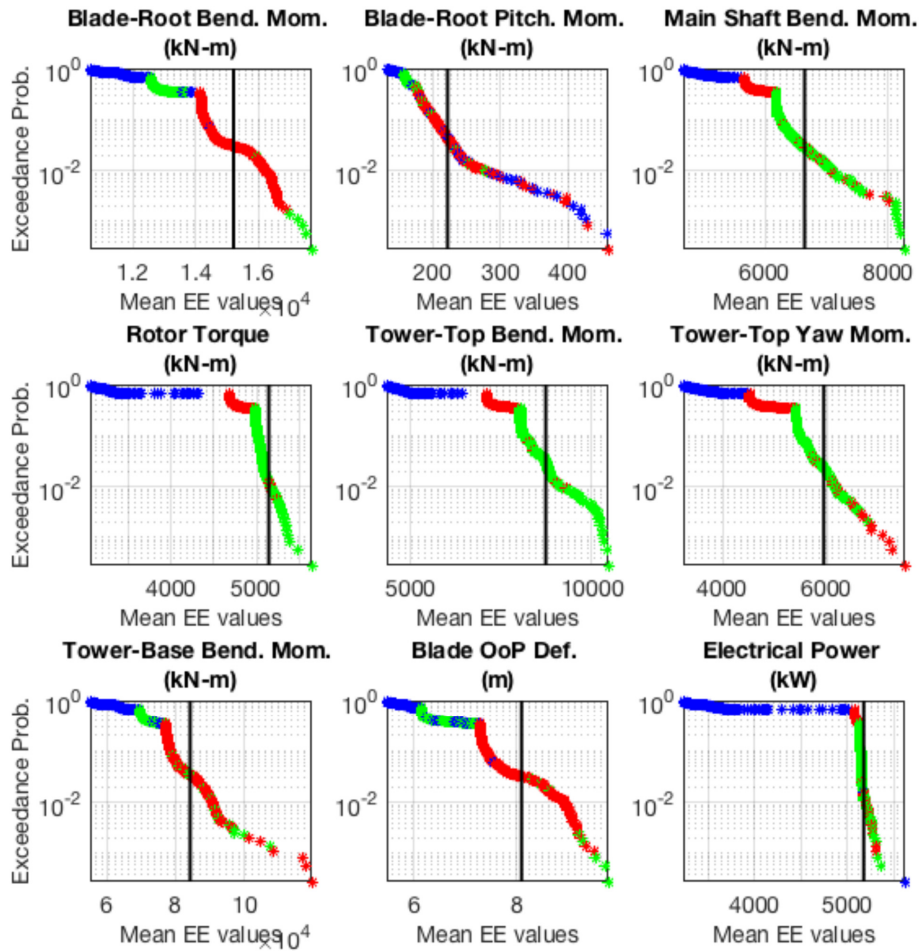


Figure 23: EE-value exceedance probability plots of ultimate loads for aeroelastic turbine parameters, across all wind speed bins, input parameters, and simulations points for all QoIs. The black line represents the defined threshold by which outliers are counted for each QoI. Color indicates wind speed bin (blue=below rated, red=near rated, green=above rated).

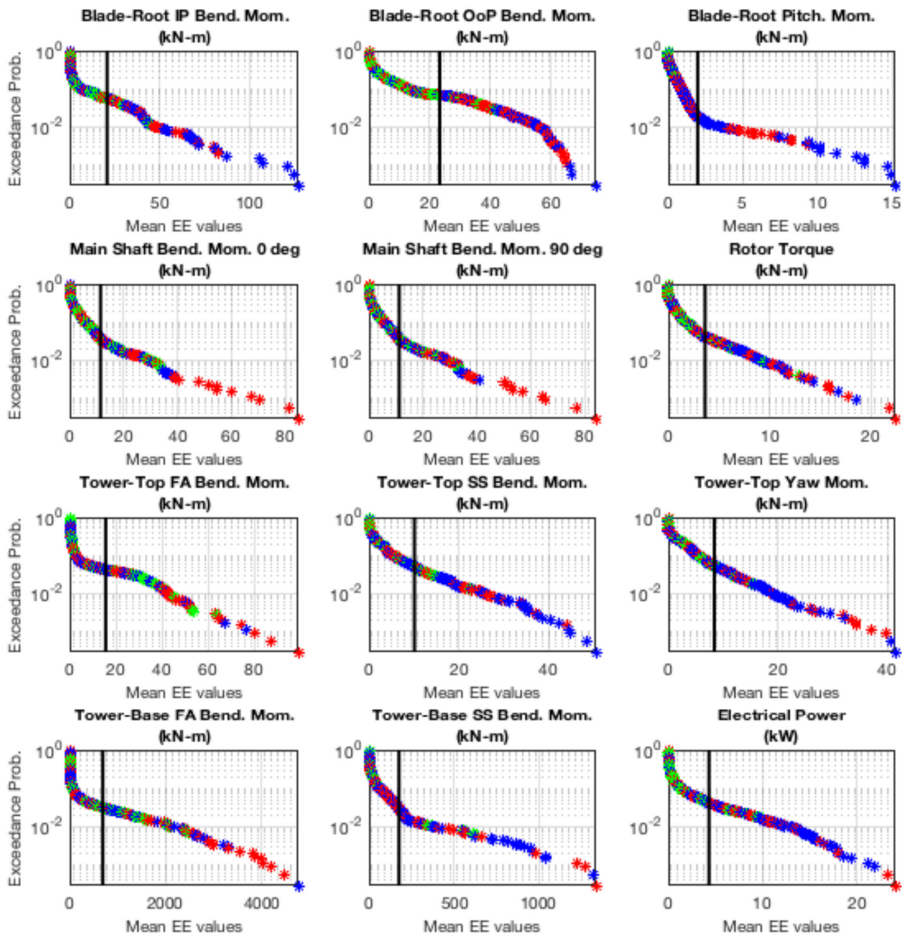


Figure 24: EE-value exceedance probability plots of fatigue loads of aeroelastic turbine parameters across all wind speed bins, input parameters, and simulations points for all QoIs. The black line represents the defined threshold by which outliers are counted for each QoI. Color indicates wind speed bin (blue=below rated, red=near rated, green=above rated).

5

Formatted: Normal
 Formatted: Normal, Space After: 0 pt

Acknowledgements

This work was authored by Alliance for Sustainable Energy, LLC, the manager and operator of the National Renewable Energy Laboratory for the U.S. Department of Energy (DOE) under Contract No. DE-AC36-08GO28308. Funding provided by Department of Energy Office of Energy Efficiency and Renewable Energy, Wind Energy Technologies Office. The views expressed in the article do not necessarily represent the views of the DOE or the U.S. Government. The U.S. Government retains and the publisher, by accepting the article for publication, acknowledges that the U.S. Government retains a nonexclusive, paid-up, irrevocable, worldwide license to publish or reproduce the published form of this work, or allow others to do so, for U.S. Government purposes.

References

1. Abdallah, G., Natarajan, A., and Sorensen, J., "Impact of Uncertainty in Airfoil Characteristics on Wind Turbine Extreme Loads," *Renewable Energy*, Vol. 75, 2015, pp. 283–300. doi:10.1016/j.renene.2014.10.009.
2. Abdallah, I., Natarajan, A., and Sorensen, J., "Assessment of extreme design loads for modern wind turbines using the probabilistic approach," DTU Wind Energy (DTU Wind Energy PhD; No. 0048(EN)), 2015.
3. Berg, J., Mann, J., and Patten, E.G., "Lidar-Observed Stress Vectors and Veer in the Atmospheric Boundary Layer," *Journal of Atmospheric and Oceanic Technology*, Vol. 30, September 2013.
4. Bulaevskaya, V., Wharton, S., Cliftons, A., Qualley, G., and Miller, W., "Wind Power Curve Modeling in Complex Terrain Using Statistical Models," *Journal of Renewable and Sustainable Energy*, vol. 7, 2015.
5. Burton, T., Jenkins, N., Sharpe, D., and Bossanyi, E., *Wind Energy Handbook*, 2011.
6. Campolongo, F., Cariboni, J., and Saltelli, A., "An Effective Screening Design for Sensitivity Analysis of Large Models," *Environmental Modelling and Software* Vol. 22, 2007, pp. 1509–1518.
7. Campolongo, F., Saltelli, A., and Cariboni, J., "From Screening to Quantitative Sensitivity Analysis. A Unified Approach," *Computer Physics Computations*, Vol. 182, 2011, pp. 978–988.
8. Clifton, A., "135-m Meteorological Towers at the NWTCC: Instrumentation, Data Acquisition and Processing," *Draft*, <https://wind.nrel.gov/MetData/Publications/>.
9. Crestaux, T., Maitre, O., and Martinez, J., "Polynomial Chaos Expansion for Sensitivity Analysis," *Reliability Engineering and System Safety*, Vol. 94, 2009, pp. 1161–1172.
10. Damiani, R. R., Hayman, G. J., and Jonkman, J., "Development and Validation of a New Unsteady Airfoil Aerodynamics Model Within AeroDyn," *AIAA SciTech Forum*, AIAA, San Diego, CA, 2016, pp. 1–21. doi:10.2514/6.2016-1007.
11. Damiani, R., personal communication, May 2018.
12. Dimitrov, N., and Berg, J., "2016 CCA: Wind2loads," *Presentation at Wind2loads Industry Webinar*, February 22nd, 2017.
13. Dimitrov, N., Natarajan, A., and Kelly, M., "Model of Wind Shear Conditional on Turbulence and Its Impact on Wind Turbine Loads," *Wind Energy*, Vol. 18, 2015, pp. 1917–1931.
14. Downey, R., "Uncertainty in Wind Turbine Life Equivalent Load due to Variation of Site Conditions," *M.Sc. Thesis Project* for the Technical University of Denmark, 2006.
15. Eggers, A., Digumarthi, R., and Chaney, K., "Wind Shear and Turbulence Effects on Rotor Fatigue and Loads Control," *Transactions of the ASME*, Vol. 125, November 2003.
16. Ehrmann, R.S., Wilcox, B., White, E. B., and et al., "Effect of Surface Roughness on Wind Turbine Performance," Tech. Rep. SAND2017-10669, Sandia National Laboratory, Albuquerque, NM, October 2017.
17. Ernst, B., and Seume, J., "Investigation of Site-Specific Wind Field Parameters and Their Effect on Loads of Offshore Wind Turbines," *Energies*, Vol. 5, 2012, pp. 3835–3855.
18. Francos, A., Elorza, F., Bouraoui, F., Bidoglio, G., and Galbiati, L., "Sensitivity Analysis of Distributed Environmental Simulation Models: Understanding the Model Behavior in Hydrological Studies at the Catchment Scale," *Reliability Engineering and System Safety*, Vol. 79, 2003, pp. 205–218.
19. Gan, Y. and et al., "A Comprehensive Evaluation of Various Sensitivity Analysis Methods: A Case Study with a Hydrological Model," *Environmental Modelling and Software*, Vol. 51, 2014, pp. 269–285.
20. Gan, Y. and et al., "A Comprehensive Evaluation of Various Sensitivity Analysis Methods: A Case Study with a Hydrological
21. Hayman, G. and Buhl, J. (2012). "MLife User's Guide for Version 1.00," NREL Technical Report, downloaded from: https://nwtcc.nrel.gov/system/files/MLife_User.pdf.

22. Holierhoek, J.G., Korterink, H., van de Pieterman, R.P., Braam, H., Rademakers, L.W.M.M., and et al. (2010). "PROTEST: Recommended Practices for Measuring in Situ the 'Loads' on Drive Train, Pitch System, and Yaw System". ECN, PROTEST project deliverable D6, D7, D8.
23. Holtslag, M., Bierbooms, W., and Bussel, G., "Wind Turbine Fatigue Loads as a Function of Atmospheric Conditions," *Wind Energy*, Vol. 19, 2016, pp. 1917–1932.
24. Huang, Y. and Pierson, D., "Identifying Parameter Sensitivity in Water Quality Model of a Reservoir," *Water Quality Research Journal of Canada*, Vol. 47, 2012, pp. 451–462.
25. IEC, "IEC 61400–1 Ed. 3. Wind Turbines – Part 1: Design Requirements," 2005.
26. IEC, "IEC 61400–5 Ed. 3. Wind Turbines – Part 5: Rotor Blades Wind Turbines," 2010.
27. Jansen, M., "Analysis of Variance Designs for Model Output," *Computer Physics Communication*, Vol. 117, 1999, pp. 35–43.
28. Jonkman, B., "TurbSim User's Guide v1.50", NREL/TP-500-46198, 2009.
29. Jonkman, J., Butterfield, S., Musial, W., and Scott, G., "Definition of a 5-MW Reference Wind Turbine for Offshore System Development," NREL/TP-500-38060, Golden, CO: National Renewable Energy Laboratory, February 2009.
30. Kalverla, P., Steeuveld, G., Ronda, R., and Holtslag, A., "An Observational Climatology of Anomalous Wind Events at Offshore Meteomast Ijmuiden (North Sea)," *Journal of Wind Engineering and Industrial Aerodynamics*, Vol. 165, 2017, pp. 86–99.
31. Kelley, N., "Turbulence-Turbine Interaction: The Bases for the Development of the TurbSim Stochastic Simulator," NREL Report TP-5000-52353, 2011.
32. Kelly, M., Larsen, G., Dimitrov, N., and Natarjan, A., "Probabilistic Meteorological Characterization for Turbine Loads," *The Science of Making Torque from Wind*, Vol. 524, 2014.
33. Koukoura, C., "Validated Loads Prediction Models for Offshore Wind Turbines for Enhanced Component Reliability," DTU Wind Energy (DTU Wind Energy PhD; No. 0026 (EN), 2014.
34. Lindelöw-Marsden, P., "Uncertainties in Wind Assessment with LIDAR," *Risø-R-1681UpWind Deliverable D1*, Risø National Laboratory for Sustainable Energy, Technical University of Denmark, January 2009.
35. Loeven, G.J.A. and Bijl, H., "Airfoil Analysis with Uncertain Geometry Using the Probabilistic Collection Method," *AIAA Structures, Structural Dynamics, and Materials Conference*, 2008.
36. Madsen, H. A., Bak, C., Paulsen, U. S., and et. al, "The DAN-AERO MW Experiments Final Report," Tech. Rep. Risø-R-1726 (EN), Risø DTU, Roskilde, Denmark, September 2010.
37. Martin, R., Lazakis, I., Barbouci, S., and Johanning, L., "Sensitivity Analysis of Offshore Wind Farm Operation and Maintenance Cost and Availability," *Renewable Energy*, Vol. 85, 2016, pp. 1226–1236.
38. Matthuas, D., Bortolotti, P., Loganathan, J., and Bottasso, C., "A Study of the Propagation of Aero and Wind Uncertainties and their Effect on the Dynamic Loads of a Wind Turbine," *AIAA SciTech Forum*, 2017.
39. Moriarty, P., Holley, W., and Butterfield, S., "Effect of Turbulence Variation on Extreme Loads Prediction of Wind Turbines," *Journal of Solar Energy Engineering*, Vol. 124, 2002, pp. 387–395.
40. Moroz, E., "Time to Upgrade the Wind Turbine Suitability Process," *Presentation at AWEA WindPower 2017*.
41. Nelson, L.D., Manuel, L., Sutherland, H.J., and Veers, P.S., "Statistical Analysis of Wind Turbine Inflow and Structural Response Data from the LIST Program," *Journal of Solar Energy Engineering*, Vol. 125, pp. 541–550, 2003.
42. "OpenFAST Documentation," November 2017. URL <http://openfast.readthedocs.io/en/master>.
43. Park, J., Manuel, L., and Basu, S., "Toward Isolation of Salient Features in Stable Boundary Layer Wind Fields that Influence Loads on Wind Turbines," *Energies*, Vol. 8, 2015.
44. Petrone, G., de Nicola, C., Quagliarella, D., Witteveen, J., and Iaccarino G., "Wind Turbine Performance Analysis Under Uncertainty," *AIAA Aerospace Sciences Meeting*, 2011.
45. Quick, J., Annoni, J., King, R., Dykes, K., Fleming, P., and Ning, A., "Optimization Under Uncertainty for Wake Steering Strategies," *Wake Conference*, Vol. 854, 2017.
46. Rinker, J., "Calculating the Sensitivity of Wind Turbine Loads to Wind Inputs Using Response Surfaces," *The Science of Making Torque from Wind*, Vol. 753, 2016.
47. Robertson, A. Sethuraman, J.; Jonkman, J.; Quick, J. "Assessment of Wind Parameter Sensitivity on Ultimate and Fatigue Wind Turbine Loads," *Presented at the American Institute of Aeronautics and Astronautics SciTech Forum*, Orlando, Florida January 8–12, 2018.
48. Saint-Geours, N. and Lilburne, L., "Comparison of Three Spatial Sensitivity Analysis Techniques," *Accuracy 2010 Symposium*.
49. Saltelli, A. and et al., *Global Sensitivity Analysis, The Primer*, 2008.
50. Santos, R. and van Dam, J. "Mechanical Loads Test Report for the U.S. Department of Energy 1.5-Megawatt Wind Turbine," NREL/TP-5000-63679, 2015.
51. Saranyasontoom, K., Manuel, L., and Veers, P.S., "A Comparison of Standard Coherence Models for Inflow Turbulence with Estimates from Field Measurements," *Journal of Solar Energy Engineering*, Vol. 126, November 2004.

52. Saranyasoontorn, K. and Manuel, L., "On the Study of Uncertainty in Inflow Turbulence Model Parameters in Wind Turbine Applications," *44th AIAA Aerospace Sciences Meeting and Exhibit*, 9–12 January 2006, Reno, Nevada.
53. Saranyasoontorn, K. and Manuel, L., "On the Propagation of Uncertainty in Inflow Turbulence to Wind Turbine Loads," *Journal of Wind Engineering and Industrial Aerodynamics*, Vol. 96, 2008, pp. 508–523.
- 5 54. Sathe, A., Mann, J., Barla, T., Bierbooms, A., and van Bussel, G., "Influence of atmospheric stability on wind turbine loads," *Wind Energy*, 2012.
55. Simani, S. and Castaldi, P., "Robust Control Examples Applied to a Wind Turbine Simulated Model," *Applied Sciences*, Vol. 8, 2017, pp. 1–28.
- 10 56. Simms, D., Schreck, S., Hand, M., and Fingersh, L., "NREL Unsteady Aerodynamics Experiment in the NASA-Ames Wind Tunnel: A Comparison of Predictions to Measurements," Tech. Rep. NREL/TP-500-29494, National Renewable Energy Laboratory, Golden, CO, June 2001.
57. Sohler, H., Piet-Lahanier, H., and Farges, J., "Analysis and Optimization of an Air-Launch-to-Orbit Separation," *Acta Astronautica*, Vol. 108, 2015, pp. 18–29.
- 15 58. Solari, G. and Piccardo, G., "Probabilistic 3-D Turbulence Modeling for Gust Buffeting of Structures," *Probabilistic Engineering Mechanics*, Vol. 16, 2001, pp. 73–86.
59. Solari, G., "Turbulence Modelling for Gust Loading," *ASCE Journal of Structural Engineering*, Vol. 113, no.7, 1987, pp. 1550–1569.
60. Sumner, T., Shephard, E., and Bogle, I., "A Methodology for Global-Sensitivity Analysis of Time-Dependent Outputs in Systems Biology Modelling," *Journal of the Royal Society Interface*, Vol. 9, 2012, pp. 2156–2166.
- 20 61. Sutherland, H., "Analysis of the Structural and Inflow Data from the LIST Turbine," Sandia National Laboratories Report, SAND2002-1838J, 2002.
62. Teunissen, H., "Characteristics of the Mean Wind and Turbulence in the Planetary Boundary Layer," *UTIAS 32*, Institute for Aerospace Studies, University of Toronto, 1970.
63. Wagner, R., Courtney, M., and Larsen, T., "Simulation of Shear and Turbulence Impact on Wind Turbine Performance," *Risø-R-Report 1722*, Jan. 2010.
- 25 64. Walter, K., Weiss, C., Swift, A., Chapman, J., and Kelley, N., "Speed and Direction Shear in the Stable Nocturnal Boundary Layer," *Journal of Solar Energy Engineering*, Vol. 131, 2009.
65. Wharton, S., Newman, J.F., Qualley, G., and Miller, W.O., "Measuring Turbine Inflow with Vertically-Profiling Lidar in Complex Terrain," *J. Wind Eng. Ind. Aerodyn.*, Vol. 142, 2015, pp. 217–231.
66. Witcher, D., "Uncertainty Quantification Techniques in Wind Turbine Design," *Presentation 2017*.
- 30 67. Ziegler, L. and Muskulus, M., "Fatigue Reassessment for Lifetime Extension of Offshore Wind Monopile Substructures," *The Science of Making Torque from Wind*, Vol. 753, 2016.

| | | |
|---|-----------------------|-----------------------------|
| Page 34: [1] Formatted | Shaler, Kelsey | 3/9/2019 11:54:00 AM |
| Font: (Default) Times New Roman | | |
| Page 34: [1] Formatted | Shaler, Kelsey | 3/9/2019 11:54:00 AM |
| Font: (Default) Times New Roman | | |
| Page 34: [1] Formatted | Shaler, Kelsey | 3/9/2019 11:54:00 AM |
| Font: (Default) Times New Roman | | |
| Page 34: [2] Formatted | Shaler, Kelsey | 3/9/2019 11:54:00 AM |
| Font: (Default) Times New Roman, Font color: Auto | | |
| Page 34: [2] Formatted | Shaler, Kelsey | 3/9/2019 11:54:00 AM |
| Font: (Default) Times New Roman, Font color: Auto | | |
| Page 34: [3] Formatted | Shaler, Kelsey | 3/9/2019 11:54:00 AM |
| Font: (Default) Times New Roman, Font color: Auto | | |
| Page 34: [3] Formatted | Shaler, Kelsey | 3/9/2019 11:54:00 AM |
| Font: (Default) Times New Roman, Font color: Auto | | |
| Page 34: [4] Formatted | Shaler, Kelsey | 3/9/2019 11:54:00 AM |
| Font: (Default) Times New Roman, Font color: Auto | | |
| Page 34: [4] Formatted | Shaler, Kelsey | 3/9/2019 11:54:00 AM |
| Font: (Default) Times New Roman, Font color: Auto | | |
| Page 34: [5] Formatted | Shaler, Kelsey | 3/9/2019 11:54:00 AM |
| Font: (Default) Times New Roman | | |
| Page 34: [5] Formatted | Shaler, Kelsey | 3/9/2019 11:54:00 AM |
| Font: (Default) Times New Roman | | |
| Page 34: [5] Formatted | Shaler, Kelsey | 3/9/2019 11:54:00 AM |
| Font: (Default) Times New Roman | | |
| Page 34: [6] Formatted | Shaler, Kelsey | 3/9/2019 11:54:00 AM |
| Font: (Default) Times New Roman, Font color: Auto | | |
| Page 34: [6] Formatted | Shaler, Kelsey | 3/9/2019 11:54:00 AM |
| Font: (Default) Times New Roman, Font color: Auto | | |
| Page 34: [7] Formatted | Shaler, Kelsey | 3/9/2019 11:54:00 AM |
| Font: (Default) Times New Roman, Font color: Auto | | |
| Page 34: [7] Formatted | Shaler, Kelsey | 3/9/2019 11:54:00 AM |
| Font: (Default) Times New Roman, Font color: Auto | | |
| Page 34: [8] Formatted | Shaler, Kelsey | 3/9/2019 11:54:00 AM |
| Font: (Default) Times New Roman | | |
| Page 34: [8] Formatted | Shaler, Kelsey | 3/9/2019 11:54:00 AM |
| Font: (Default) Times New Roman | | |
| Page 34: [8] Formatted | Shaler, Kelsey | 3/9/2019 11:54:00 AM |
| Font: (Default) Times New Roman | | |
| Page 34: [9] Formatted | Shaler, Kelsey | 3/9/2019 11:54:00 AM |
| Font: (Default) Times New Roman, Font color: Auto | | |
| Page 34: [9] Formatted | Shaler, Kelsey | 3/9/2019 11:54:00 AM |

| | | |
|---|-----------------------|-----------------------------|
| Page 34: [19] Formatted | Shaler, Kelsey | 3/9/2019 11:54:00 AM |
| Font: (Default) Times New Roman, Font color: Auto | | |
| Page 34: [19] Formatted | Shaler, Kelsey | 3/9/2019 11:54:00 AM |
| Font: (Default) Times New Roman, Font color: Auto | | |
| Page 34: [20] Formatted | Shaler, Kelsey | 3/9/2019 11:54:00 AM |
| Font: (Default) Times New Roman | | |
| Page 34: [20] Formatted | Shaler, Kelsey | 3/9/2019 11:54:00 AM |
| Font: (Default) Times New Roman | | |
| Page 34: [20] Formatted | Shaler, Kelsey | 3/9/2019 11:54:00 AM |
| Font: (Default) Times New Roman | | |
| Page 34: [21] Formatted | Shaler, Kelsey | 3/9/2019 11:54:00 AM |
| Font: (Default) Times New Roman, Font color: Auto | | |
| Page 34: [21] Formatted | Shaler, Kelsey | 3/9/2019 11:54:00 AM |
| Font: (Default) Times New Roman, Font color: Auto | | |
| Page 34: [22] Formatted | Shaler, Kelsey | 3/9/2019 11:54:00 AM |
| Font: (Default) Times New Roman, Font color: Auto | | |
| Page 34: [22] Formatted | Shaler, Kelsey | 3/9/2019 11:54:00 AM |
| Font: (Default) Times New Roman, Font color: Auto | | |
| Page 34: [23] Formatted | Shaler, Kelsey | 3/9/2019 11:54:00 AM |
| Font: (Default) Times New Roman, Font color: Auto | | |
| Page 34: [23] Formatted | Shaler, Kelsey | 3/9/2019 11:54:00 AM |
| Font: (Default) Times New Roman, Font color: Auto | | |
| Page 34: [24] Formatted | Shaler, Kelsey | 3/9/2019 11:54:00 AM |
| Font: (Default) Times New Roman, Font color: Auto | | |
| Page 34: [24] Formatted | Shaler, Kelsey | 3/9/2019 11:54:00 AM |
| Font: (Default) Times New Roman, Font color: Auto | | |
| Page 34: [25] Formatted | Shaler, Kelsey | 3/9/2019 11:54:00 AM |
| Font: (Default) Times New Roman, Font color: Auto | | |
| Page 34: [25] Formatted | Shaler, Kelsey | 3/9/2019 11:54:00 AM |
| Font: (Default) Times New Roman, Font color: Auto | | |
| Page 34: [26] Formatted | Shaler, Kelsey | 3/9/2019 11:54:00 AM |
| Font: (Default) Times New Roman, Font color: Auto | | |
| Page 34: [26] Formatted | Shaler, Kelsey | 3/9/2019 11:54:00 AM |
| Font: (Default) Times New Roman, Font color: Auto | | |